INTEGRATED RESERVOIR STUDY OF THE MONUMENT NORTHWEST FIELD: A WATERFLOOD PERFORMANCE EVALUATION

A Thesis

by

MOSES ASUQUO NDUONYI

Submitted to the Office of Graduate Studies of
Texas A&M University
in partial fulfillment of the requirements for the degree of

MASTER OF SCIENCE

December 2007

Major Subject: Petroleum Engineering

INTEGRATED RESERVOIR STUDY OF THE MONUMENT NORTHWEST FIELD: A WATERFLOOD PERFORMANCE EVALUATION

A Thesis

by

MOSES ASUQUO NDUONYI

Submitted to the Office of Graduate Studies of
Texas A&M University
in partial fulfillment of the requirements for the degree of

MASTER OF SCIENCE

Approved by:

Chair of Committee,	David S. Schechter
Committee Members,	Robert A. Wattenbarger
	Wayne Ahr
Head of Department,	Stephen A. Holditch

December 2007

Major Subject: Petroleum Engineering

ABSTRACT

Integrated Reservoir Study of the Monument Northwest Field: A Waterflood Performance Evaluation. (December 2007)

Moses Asuquo Nduonyi, B.Eng., University of Port Harcourt, Nigeria

Chair of Advisory Committee: Dr. David S. Schechter

An integrated full-field study was conducted on the Monument Northwest field located in Kansas. The purpose of this study was to determine the feasibility and profitability of a waterflood using numerical simulation. Outlined in this thesis is a methodology for a deterministic approach. The data history of the wells in the field beginning from spud date were gathered and analyzed into information necessary for building an upscaled reservoir model of the field. Means of increasing production and recovery from the field via a waterflood was implemented.

Usually, at the time of such a redevelopment plan or scheme to improve field performance, a tangible amount of information about the reservoir is already known. Therefore it is very useful incorporating knowledge about the field in predicting future behavior of the field under certain conditions. The need for an integrated reservoir study cannot be over-emphasized. Information known about the reservoir from different segments of the field exploration and production are coupled and harnessed into developing a representative 3D reservoir model of the field.

An integrated approach is used in developing a 3D reservoir model of the Monument Northwest field and a waterflood is evaluated and analyzed by a simulation of the reservoir model. From the results of the reservoir simulation it was concluded that the waterflood project for the Monument Northwest field is a viable and economic project.

DEDICATION

I dedicate this work to my parents, Nkoyo and Etim Nduonyi, for the encouragement and love they gave me. I am grateful they believed in me.

ACKNOWLEDGEMENTS

I would like to thank my committee chair, Dr. David Schechter, and my committee members, Dr. Robert Wattenbarger and Dr. Wayne Ahr for their guidance and support throughout the course of this research.

I would also like to thank my mentor, Mr. William Johnson, a Reservoir Engineering Consultant in Kansas for teaching me how to "tie the ropes" the practical way incorporating the inadequacy of the real world. I am very grateful to Mr. Thomas Tan of Petrostudies for donating a free license of EXODUS software to the Petroleum Engineering Department for use in the successful completion of this project. The software proved to be an invaluable tool.

I thank the faculty and staff of the Petroleum Engineering Department and the Geology Department; my association with them has been very rewarding in many ways. I would specifically thank Dr. Christine Economides for teaching me well testing; I could not have learned it better.

I would also thank Dr. Alan Byrnes of the University of Kansas for sharing knowledge and information. Thank you for being there always.

Finally, I would like to thank my parents and my brothers for their patience, love, and support. We all did this project together.

TABLE OF CONTENTS

LIST OF FIGURES

FIGURE Page

FIGURE Page

LIST OF TABLES

CHAPTER I

INTRODUCTION

Improving the performance and recovery of a field is usually attempted particularly in oilfields with normal depletion recoveries running as low as 10-15%. It is very critical that this attempt be positive because the outcome of subsequent trials depends greatly on a previous attempt. Integrated reservoir study by itself is quite ambiguous but associating an integrated reservoir study with a purpose ultimately defines the study and its applicability. An attempt to improve the field performance and recovery of the Monument Northwest (NW) field by water injection is carried out in this thesis.

The data necessary for this analysis included a drilling and completion report of each well, drill stem tests data, log data, and production data. This data was analyzed and integrated with structure and isopach maps obtained from geophysical interpretation of three-dimensional seismic surveys. The primary tools used for this analysis were Exodus 3D-3 Phase simulator, Geographix Suite and the Fekete F.A.S.T software suite.

This thesis report will be divided into segments which would detail the reservoir description and petrophysical evaluation, the pressure evaluation, the reservoir model development, the reservoir history match, and finally the simulation of various waterflooding scenarios for performance evaluation, recovery improvement and economic analysis. In as much as these segments seem to be separate, they were run

---

This thesis follows the style of the SPE Journal.

concurrently to deduce and intersect information from various segments to ensure a valid deterministic model.

Previous Work

The ability to predict the size, shape and orientation of a reservoir rock body with respect to the basin of deposition and the structure is a very important skill. Petroleum geologists have studied various carbonate rocks with a view of this and tremendous progress has been made regarding the understanding of carbonate rocks[1].

Folk and Dunham classified carbonates based on its textural maturity and its grain properties by associating it with its environmental properties such as energy level of deposition[2]. Folk and Dunham further subdivided carbonate rocks into four major groups based upon the relative proportions of coarse clastic grains and lime mud. Rock properties play an important role in the geological description of carbonate reservoirs but it is necessary to create a geological concept using descriptive rock properties, porosity, permeability and borehole log characteristics[3]. Ahr[4] suggested a geological model which links total porosity, pore types, permeability and some other descriptive rock properties to depositional, diagenetic, and structural configuration; this will help us get a flow unit characterization which is an indicator of the quality and continuity of the reservoir.

Integrated reservoir study is done at some point in a field's life whether or not this is documented. The processes and methods may vary but it is practically the same in logic and principle. This is the first integrated reservoir study performed on the Monument Northwest field in Logan County. Previous work done on this field involved the petrophysical characterization of this field, which I have incorporated within as a segment of this whole study.

Byrnes and Bhattacharya[5] worked extensively on cores from shallow shelf carbonate lithologies to characterize petrophysical and relative permeability characteristics. The authors conducted experiments on some 950 core plugs from the shallow shelf carbonate fields across Kansas mainly from the Lansing group. The authors related the saturations and porosity using a trapping constant. Power law and logarithmic relationships of petrophysical properties of the cores were defined using this trapping characteristic.

In any complete integrated reservoir study, different phases would have to be dealt with separately and concurrently. This will involve a detailed geologic analysis and characterization of the reservoir and rock properties, characterizing reservoir fluid properties for material balance calculations, developing a three-dimensional reservoir simulation model in order to match the production and pressure histories and finally, developing and implementing different reservoir management and production strategies to optimize recovery from the field[6].

CHAPTER II

GEOLOGICAL AND PETROPHYSICAL EVALUATION

It is important to type the rock first in any petrophysical analysis[3]. Data used for the petrophysical analysis of the Monument NW field include the drilling report and wireline logs. A digital log database was developed which was a suite containing a spontaneous potential, gamma ray, caliper, resistivity and porosity logs. This log suite was then interpreted using the Archie interpretation while still corresponding with the drilling report concurrently. A simple flowchart describing the petrophysical evaluation used in the analysis is presented in Figure 1.

Some characteristics indirectly inferred from our log analysis include secondary porosity and wettability characteristics. These properties are useful on a qualitative basis. From a standard SWS CP-1c chart shown in Figure 2 which identifies formation based on its bulk density we identified a carbonate formation. This is simply inferred from an estimate of the bulk densities which are above 2.7 g/cm^3 at the compared porosity. These represent different grain structures ranging from mudstone to wackestone when compared against log-derived porosity. From the field geology, it was inferred that the diagenesis of the field occurred after the deposition but before the migration and accumulation of hydrocarbons.

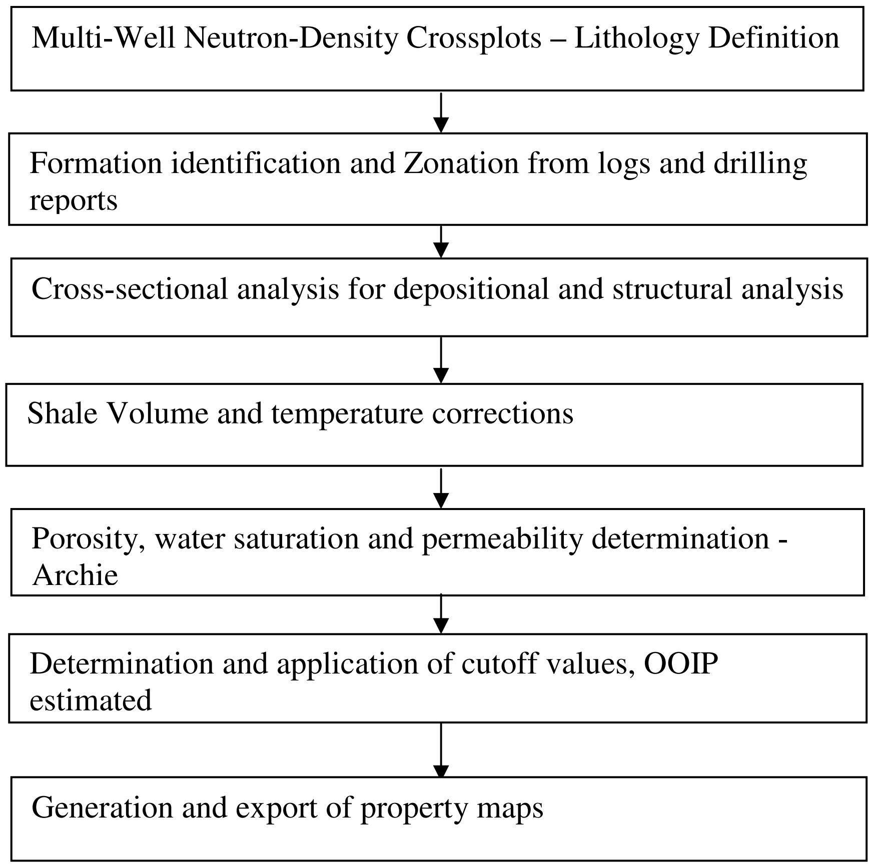

Figure 1: Flowchart showing sequence used in petrophysical evaluation.

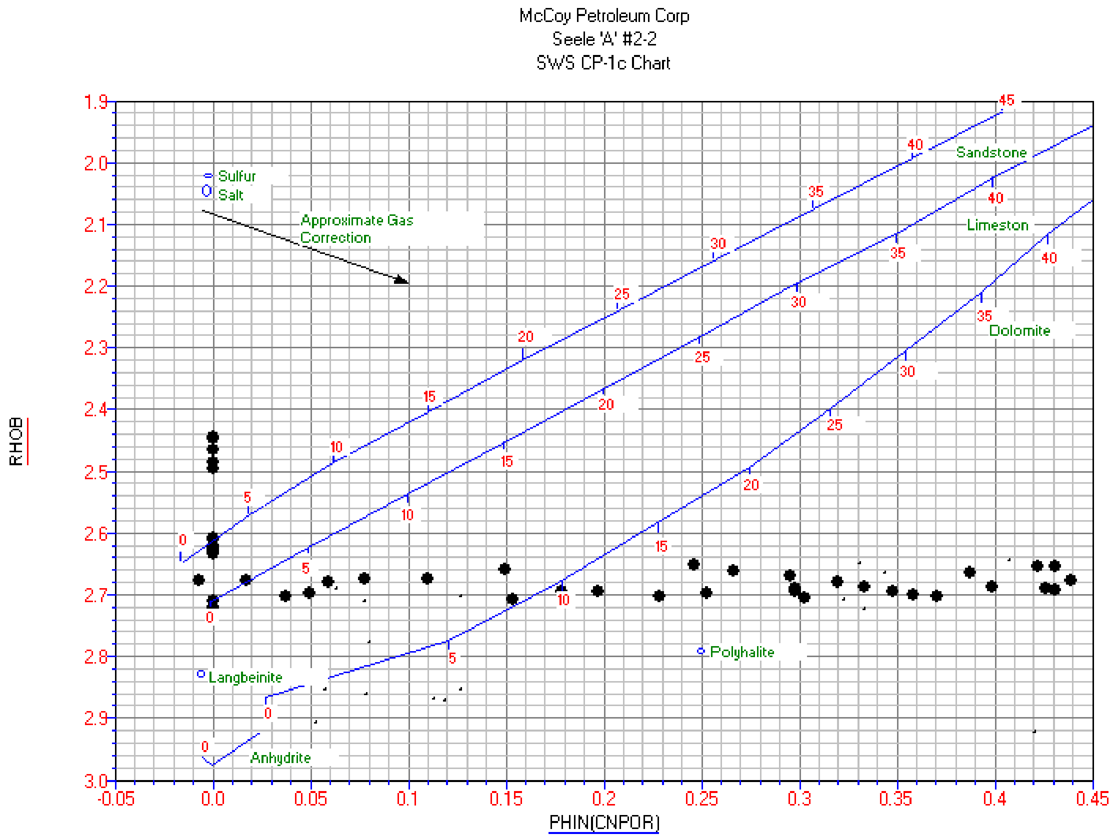

Figure 2: Multi-well neutron-density crossplot for lithology identification.

Following this hypothesis is the fact that with dolomitization comes evaporites, volume shrinkage, and water-expulsion[7]. This process occurred sequentially from layer to layer. After a subsequent layer is deposited on an older layer which is undergoing or has undergone diagenetic effects, the water expelled is moved upward by buoyancy. With this depositional history we can tie in the migration and accumulation time to be during the diagenesis of the H-Zone (the topmost layer) which is basically deduced from the fact that this zone has an aquifer. The aquifer is due to the trapped water in that layer. The evaporites and the overlying shales formed the trap for the hydrocarbons.

With this depositional history set, some established facts include that the rocks are water-wet, each layer will be heterogeneous in permeability and porosity due to the fact that diagenesis tend to reduce and redistribute porosity and permeability. More so we expect a drastic and irregular permeability distribution.

Following the general lithology identification in the flowchart is the picking of formations (see Figure 3) and cross-sectional analysis. These are marked on from the logs by getting information from drilling reports and verified by signatures on the gamma ray logs and the caliper log which showed a slight size reduction due to mudcake. Facies sequencing from gamma ray logs alone are very insignificant as compared to a sandstone formation[8]. A stratigraphic and structural column of a cross-section is made to help explain geologic and depositional trends of the environment. This field is in a low-energy terrestrial environment with Phanerozoic sedimentary rocks. These environments are dominated by mud-rich facies, where much of the porosity is diagenetic in nature. The cross-section selected is an increasing path from well to well across the field taken in a diagonal from Thrasher B#1 to Anderson C#1. We observe a gently sloping depositional environment usually associated with lacustrine deposits[9]. The cross-sections are analyzed in two segments shown in Figures 4 and 5.

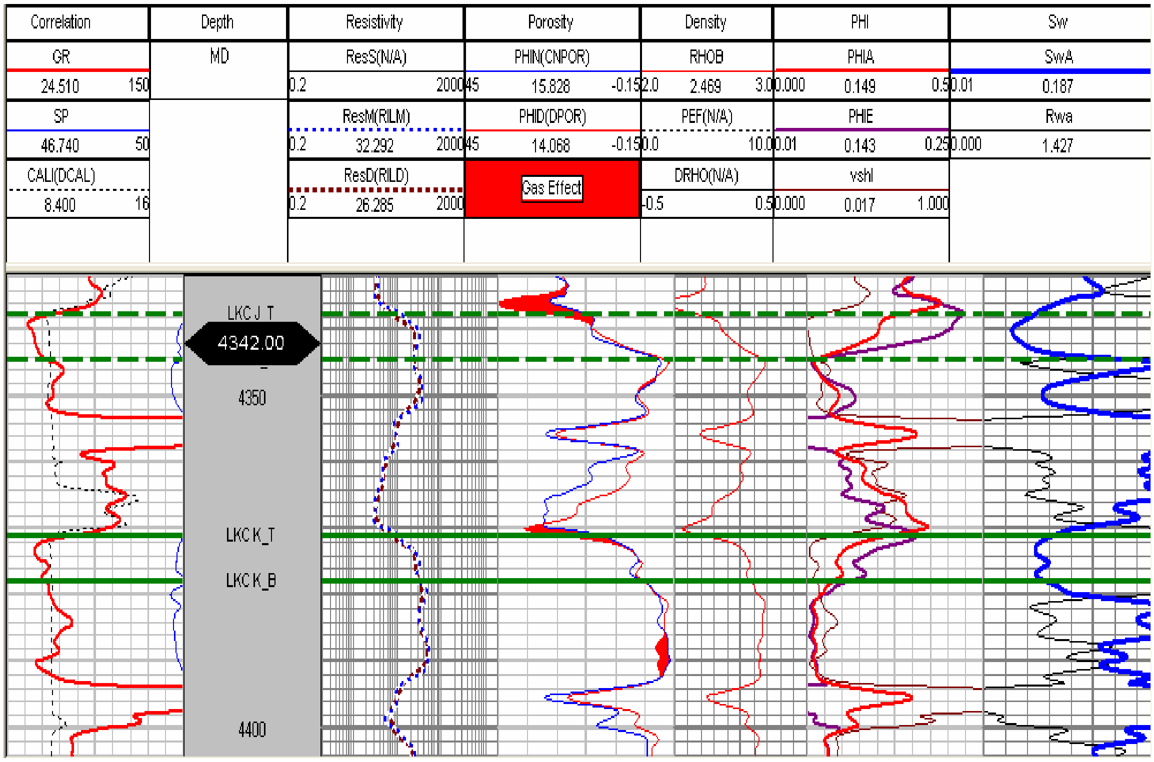

Figure 3: Log template showing formation picks. J-Zone is shown in hatched green lines and the K-Zone is shown in the full green lines.

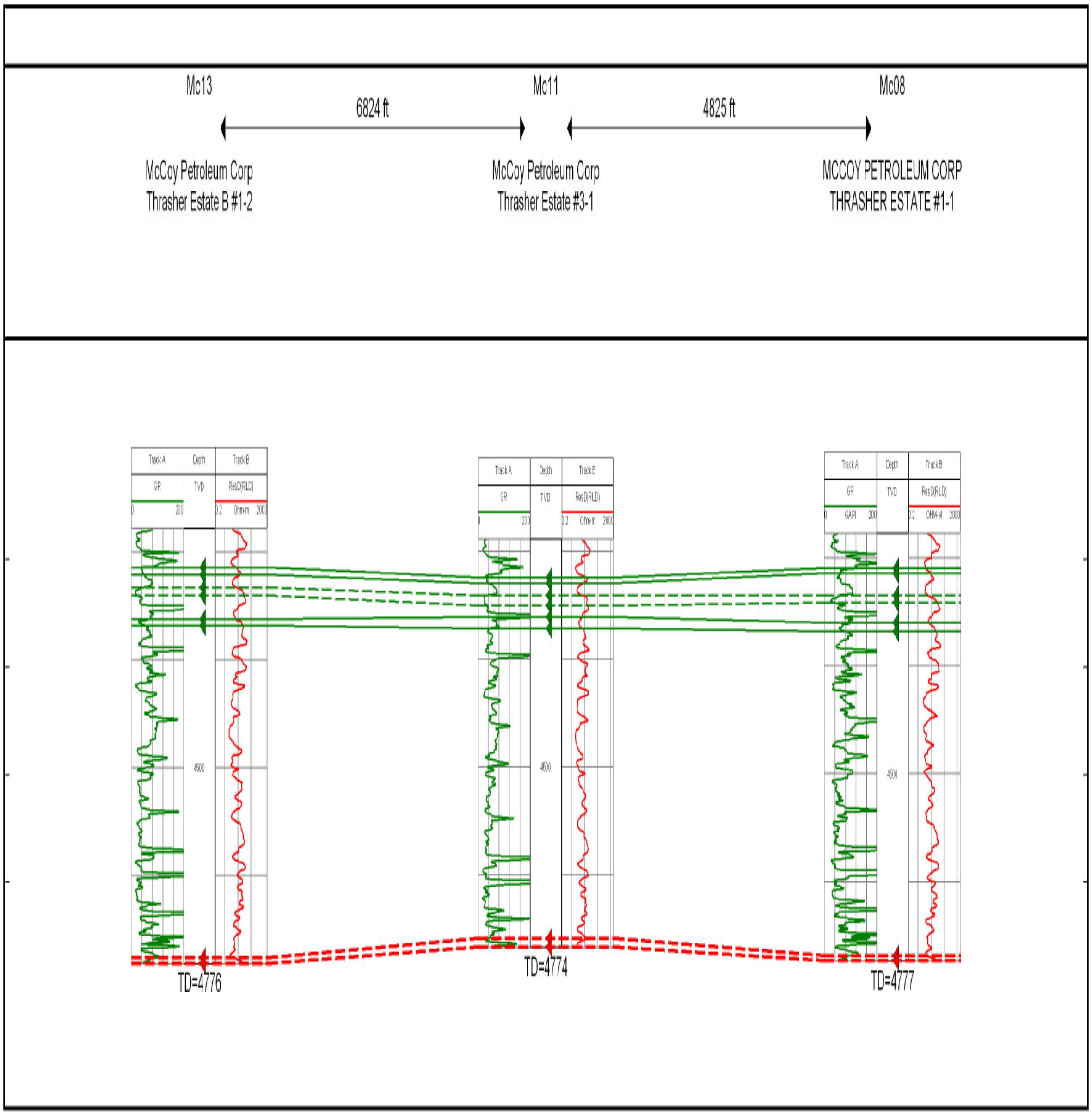

Figure 4: Cross-sectional view between Thrasher B#1 to Thrasher A#1. From top to bottom we see zones I, J, K and the Johnson zone respectively. This is relatively flat with respect to sea-level.

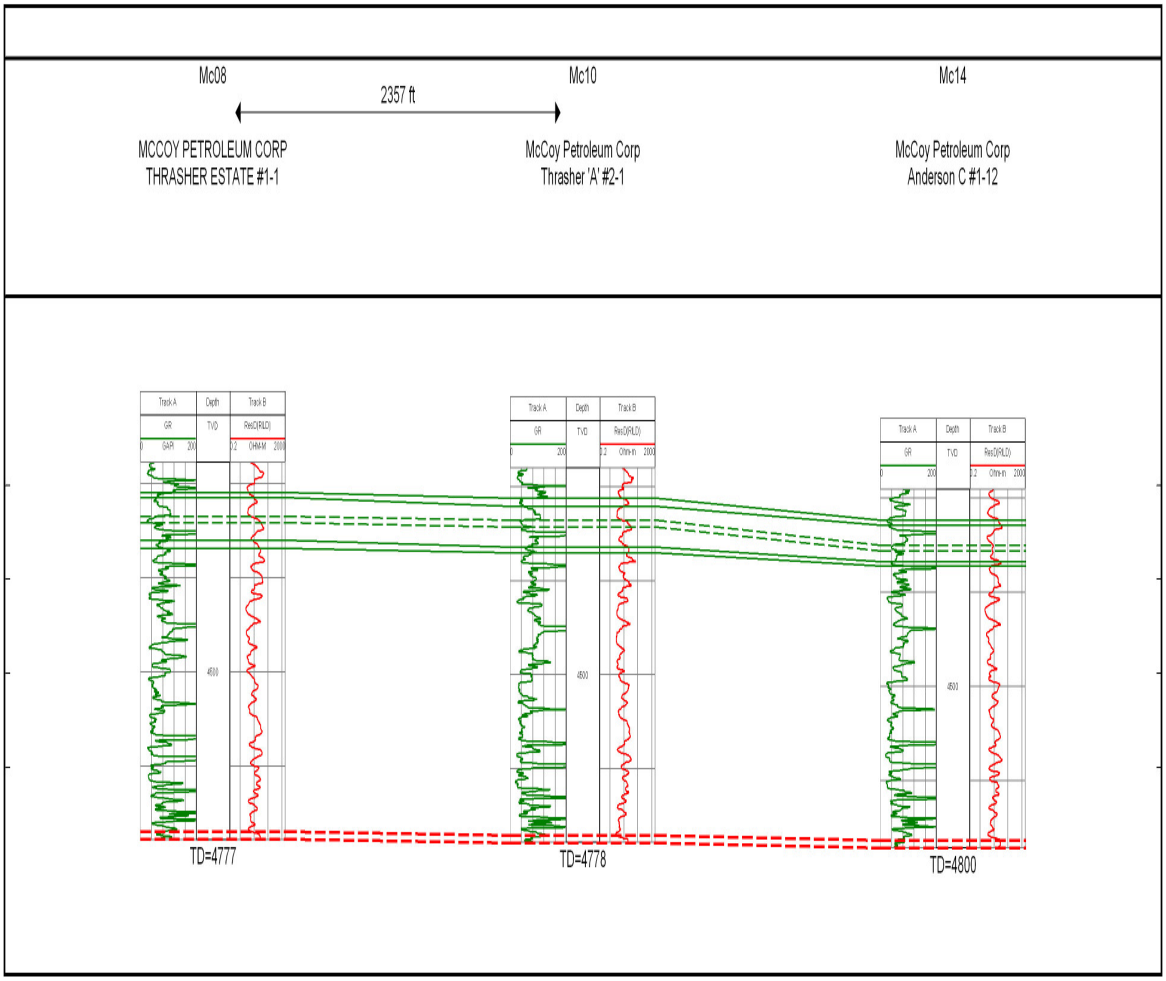

Figure 5: Cross-sectional view between Thrasher A#1 to Anderson C#1. From top to bottom we see zones I, J, K and the Johnson zone respectively

The typical Archie interpretation is used for the petrophysical analysis. This will basically quantify porosity, net pay thickness and water saturation for identified zones. The effect of shaliness on measured readings needs to be corrected before using log data for analysis[3]. This is done by quantifying the shale volume. Shale volume was evaluated using the gamma ray index and the steiber shale correction factor. This was used because it is more conservative and goes well with younger rocks. The gamma ray index and the Steiber equations are given as equations 1 and 2 respectively:

$$V_{sh\_GR} = \frac{Min(1, Max(0, (GR - GR_{c\ln})}{(GR_{shl} - GR_{c\ln})} \tag{1}$$

$$V_{sh\_ST} = \frac{V_{sh\_GR}}{3 - 2 * V_{sh\_GR}} \tag{2}$$

Gamma ray values of 20 API and 120 API were used for GR_{cln} and GR_{shl} respectively. The shale volume calculation is used as a correction for the actual log measurements as well as gives us a general trend of the vertical lithology distribution. Porosity was determined from log measurments of neutron and density porosities. A preferential average for porosity was evaluated as:

$$PHIA = \frac{PHIN + PHID}{2} \qquad \text{For PHIN} \leq 0.2 \tag{3}$$

$$PHIA = \frac{3 * PHID + 2 * PHIN}{5} \qquad \text{For PHIN} > 0.2 \tag{4}$$

This was corrected for shaliness by

$$PHIE = PHIA - (PHIA_{sh} * V_{sh\_ST}) \tag{5}$$

The evaluation of water saturation by any means needs the proper evaluation of the formation water resistivity[5]. The formation water resistivity was determined by two methods. The apparent resistivity method and the pickett plot method was used. These two methods were used since they utilize different data resources to an extent. The formation resistivity was determined to be 0.06 ohm-meter. The Archie equation for determining water saturation is given in Equation 6 as[3]:

$$S_w = \left(\frac{a * R_w}{\phi^m R_t} \right)^{\frac{1}{n}} \tag{6}$$

The Archie parameters a, m and n were obtained from the pickett plot by estimating one parameter and the other two parameters are obtained. Given no core data, it is safe to assume the saturation exponent as 2 which is the value used in most reservoirs. Table 1 shows values obtained from Pickett plot analysis.

Table 1: Archie parameters.

Archie Parameter	**Value**
a	1
m	1.6
n	2

Water saturation was obtained as a function of depth and average values along with the thicknesses of the identified payzones are indicated in Table 2.

Table 2: Evaluated properties from log analysis

#	Well Name	Zone Name	pay height, ft	Porosity	Sw
1	Thrasher Estate A#1-1	H-Zone	8	0.095	0.44
		I-Zone	9	0.07	0.52
		J-Zone	7	0.08	0.37
		K-Zone	8	0.06	0.46
		Johnson	5	0.054	0.5
2	Thrasher Estate A#2-1	H-Zone	7.1	0.12	0.36
		I-Zone	7	0.05	0.56
		J-Zone	5.6	0.06	0.45
		K-Zone	6	0.05	0.48
		Johnson	4	0.06	0.41
3	Thrasher Estate A#3-1	H-Zone	8	0.11	0.45
		I-Zone	7	0.09	0.45
		J-Zone	6.3	0.11	0.3
		K-Zone	5	0.09	0.42
		Johnson	4.6	0.08	0.4
4	Thrasher Estate #4-1	H-Zone	5.5	0.1	0.31
		I-Zone	5.1	0.07	0.43
		J-Zone	9.1	0.15	0.22
		K-Zone	10.7	0.07	0.36
		Johnson	6	0.06	0.37
5	Seele A#1-1	H-Zone	5	0.14	0.26
		I-Zone	5.5	0.07	0.4
		J-Zone	7.1	0.16	0.23
		K-Zone	6.5	0.14	0.28
		Johnson	6	0.06	0.43

Table 2 shows a summary of petrophysical quantities useful in evaluating oil-in-place from a petrophysical view point. These values are calculated over an area equivalent to an area analysed by a geologist and the computed reserves compared. The compared values are not equal but of the same order. The values in Table 2 are computed as an average for the well from values in all layers.

CHAPTER III

DRILL STEM TESTING

Drill stem testing is conducted during the drilling phases of the well. This is the pressure and flow evaluation of an indicated pay zone. An indicated pay zone is a zone determined by a well site geologist either from a previous geophysical evaluation or from drilling mud shows to be a potential zone of hydrocarbon accumulation. A good drill stem test yields a sample of the type of reservoir fluid present, an indication of flow rates, a measurement of the static and flowing bottom-hole pressure, an estimate of near-wellbore formation permeability, skin factor and static reservoir pressure[10].

Drill stem tests are pulsed tests[10]. These are pulsed in the sense that flow to the surface is usually not appropriate since completion and production equipment is not yet installed but the total fluid volumes must be known to evaluate the drill stem test properly.

The test starts by opening the bottom-hole valve of the drill stem test equipment allowing formation fluids to enter into the drill string. The first flow period is usually short and is seen as a reservoir clean up[10]. The well is then shut-in and then opened again for a second time for a longer period and then finally shut-in. During the flow and shut-in periods, the drill stem test equipment measures the bottom-hole pressure and fluid withdrawal at the surface is measured for volumetric calculation.

Analysis of drill stem data was done very carefully with a software application that analyses the first and second build up using rigorous welltest techniques. The flow segments are usually not analyzed with respect to pressure for two reasons being that the rates are usually not known, and also the pressure recorded by the DST equipment usually builds (particularly in oil reservoirs) with flow due to an increasing hydrostatic column while a normal drawdown analysis goes with a pressure drop[11].

Ideally, pressures from the two build-up phases are analyzed and extrapolated to obtain extrapolated pressure and initial reservoir pressure. The flow segment is analyzed to deduce rate information used in build-up test analysis. For this project, an average rate is used as a constant rate. From an analysis of the first and second build-up, reservoir depletion can be detected if extrapolated pressures from the two test segments do not correspond and the pressure has completed building up in both segments. This was not observed in the drill stem tests analyzed which meant at the field had potential at the time of completion of the wells. The importance of a drill stem test can be summarized by the following points:

- Evaluation of pressure, permeability and skin of an indicated pay interval.
- Evaluation of reservoir fluids in an indicated pay interval.
- Determination of completion details for an indicated pay interval.
- Evaluation of reservoir characterization (natural fractures)[12].

From the mathematical theory behind the test, the well known diffusivity equation in radial coordinates and dimensionless variables assuming a constant rate at the well can be expressed as[10]:

$$\frac{\partial^2 p_D}{\partial r_D^2} + \frac{1}{r_D}\frac{\partial p_D}{\partial r_D} = \frac{\partial p_D}{\partial t_D} \tag{7}$$

$$p_D(r_D, 0) = 0 \tag{8}$$

$$\lim_{r_D \to \infty} p_D(r_D, t_D) = 0 \tag{9}$$

$$p_{wD}(0_+) = 1 \tag{10}$$

Equations 8-10 are boundary conditions. The wellbore pressure and the reservoir pressure are coupled by the the Van Everdingen and Hurst skin effect[10] as

$$p_{wD}(t_D) = [p_D(r_D, t_D) - s r_D \frac{\partial p_D}{\partial r_D}]_{r_D=1} \tag{11}$$

Correa and Ramey used these equations to express the DST problem by introducing a piecewise unit step function for the wellbore storage. The wellbore storage coefficient for the production phase, C_{fD} is defined as the volume of fluid accumulated in the wellbore per unit change in wellbore pressure. Essentially, the relationship is given as

$$[(1 - H_t)C_{fD} + H_t C_{sD}]\frac{dp_{wD}}{dt_D} - [r_D \frac{\partial p_D}{\partial r_D}]_{r_D=1} = 0,\ t_D > 0 \tag{12}$$

where H_t is a unit-step function and C_{sD} is the static wellbore storage. The main difference between C_{fD} and C_{sD} is the relationship between the fluid compressibility and pressure. For slightly compressible fluids (oil) these are approximately the same values.

Equation 12 is solved using laplace transforms and appropriate boundary conditions, Correa and Ramey obtained the solution as:

$$p_{wD}(t_D) = C_{sD} P_D(s, C_{sD}, t_D) + (C_{sD} - C_{fD}) \int_0^t P_D(s, C_{sD}, t_D - \tau_D) p_{wD}'(\tau_D) d\tau_D \qquad (13)$$

Equation 13 holds the fact that as the flow time goes to zero, the integral term vanishes and the result converges to the "slug test" solution used in groundwater analysis. This poses a practical issue that the flow periods should be kept to a minimum with respect to the shut-in times for a proper DST analysis.

Equation 13 can be represented in dimensional form as

$$p_w(t) = p_i - m_c \frac{t_p}{t_p + \Delta t} \qquad (14)$$

Where the slope m_c is defined as

$$m_c = \frac{q\mu}{4\pi kh} \left[1 + \frac{C_s(p_i - p_{wf})}{qt_p} \right] \qquad (15)$$

and is representative of the flow regime of the pressure transient. The skin effect is calculated from

$$s = 0.5\log_e[\frac{C_D e^{2s}}{C_{fD}}] \tag{16}$$

Figure 6 shows a DST analyzed for one of the zones in one of the wells in the field using a proprietary software called Fekete FAST™. DST analyses were carried out in all zones whether or not these zones were completed. These provided information such as initial pressure and permeability shown in Tables 3 and 4 which were used to calibrate the reservoir model.

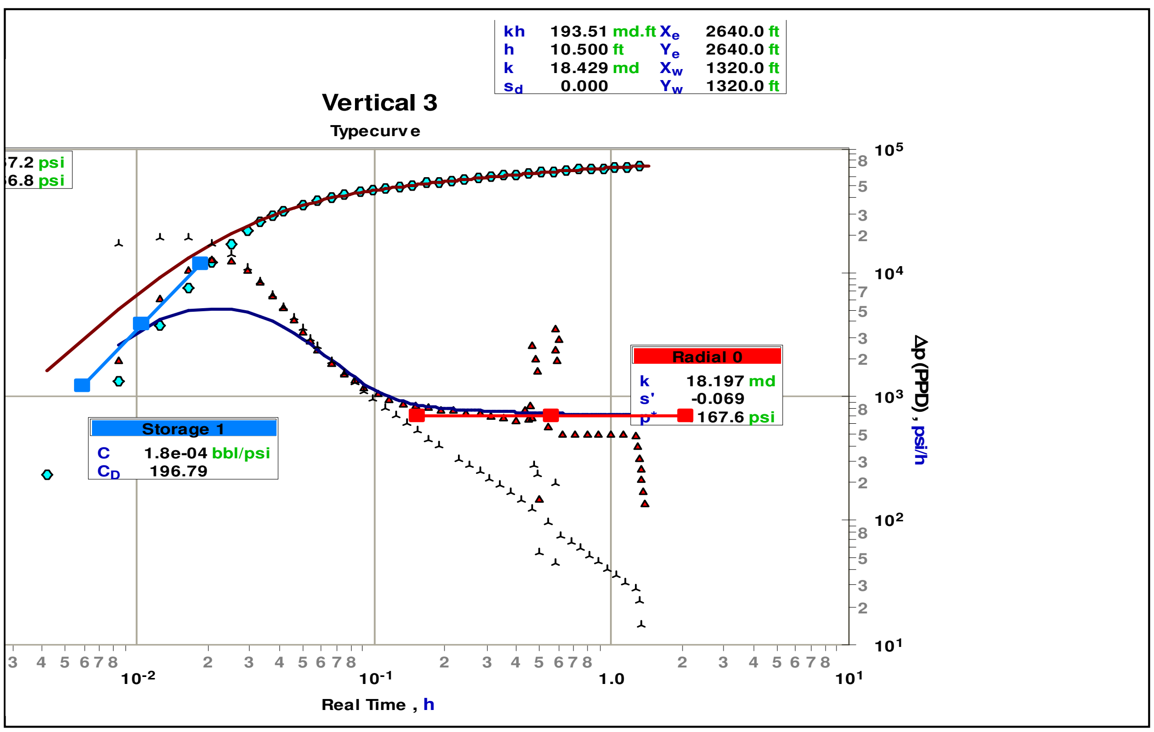

Figure 6: A typical drill stem test analysis plot. This shows the wellbore storage effect, some non-reservoir effect(a), and the infinite acting radial flow.

Table 3: DST results of 6 wells analyzed using commercial software. Results follow irregular trends as suggested by geological history.

Well Name	Date Completed	Zonal DST Analysis			
		Zone Name	Pressure, psi	Permeability, md	Skin
Thrasher A#1	4/11/2002	H	1285	181.5	0
		I	1335	1479	0.6
		J	1370	258.9	2.5
		K	1265	8.7	2.9
		Johnson	412	5.8	-2.5
Thrasher A#3	10/4/2002	H	1290	26.1	-2.2
		I	727	74.5	14
		J	812	178	2.4
		K	1226	15	-1.5
		Johnson	506	53	-3.4
Thrasher A#2	10/7/2002	H	745	4.5	-1
		I	683	33	18.3
		J	DST fault	N/A	N/A
		K	1113	5.3	0.5
		Johnson	423	7.8	-1.5
Thrasher A#4	1/6/2003	H	1228	17.1	-0.6
		I	278	258.4	4.2
		J	350	180	2.2
		K	1022	17.8	-3
		Johnson	520	94.5	-2
Seele A#1	2/11/2003	H	906	160	0
		I	291	124	7
		J	331	165	0
		K	1146	10.6	1.6
		Johnson	1130	9	-1.3
Thrasher B#1	2/12/2003	H	947	112	1.4
		I	402	6.5	5.2
		J	300	360	2.8
		K	1145	87	3
		Johnson	1050	46	-1.9

Table 4: DST results of wells analyzed using commercial software. The remaining 5 wells producing from the reservoir is shown mostly in order of DST analysis than chronologically.

Well Name	Date Completed	Zonal DST Analysis			
		Zone Name	Pressure, psi	Permeability,md	Skin
Seele A#2	3/14/2003	H	775	5.2	-1.5
		I	508	31	1
		J	508	31	1
		K	DST fault	N/A	N/A
		Johnson	DST fault	N/A	N/A
Seele A#3	3/27/2002	H	906	19	1
		I	308	250	1
		J	308	250	1
		K	540	344	7
		Johnson	486	108	-2
Thrasher B#2	5/3/2003	H	DST fault	N/A	N/A
		I	DST fault	N/A	N/A
		J	400	365	0.8
		K	683	210	20
		Johnson	605	72	-2
Anderson C#1	4/12/2003	H	N/A	N/A	N/A
		I	1207	336	-0.2
		J	1247	22	3.7
		K	1166	18	0
		Johnson	508	115	-1.25
Anderson C#3	2/3/2004	H	N/A	N/A	N/A
		I	230	N/A	N/A
		J	230	N/A	N/A
		K	N/A	N/A	N/A
		Johnson	N/A	N/A	N/A

Columns with N/A means not available, meaning either that the DST was mot measured in that zone or had un-interpretable data.

CHAPTER IV

RESERVOIR MODEL DEVELOPMENT

A reservoir simulation model is a mathematical (mostly numerical) representation of a petroleum reservoir[6]. A simulation model is built to represent an oil and gas reservoir in its size, shape and physical characteristics. The physical characteristics usually represented include but is not limited to pressure, fluid saturations, reservoir porosity, permeability, relative permeability, and influence functions.

Data gathering usually precedes reservoir model construction. Data gathered from different sources must be coherent before being incorporated into a model[6]. This helps the modeling process to be direct as it is usually the case in deterministic modeling. In achieving a good reservoir model we applied strict reservoir engineering sense while honoring geology and preserving petrophysical analysis. Following the reservoir model development is the validation which is principally done by a well known tool called history matching.

Deterministic Modeling

Deterministic modeling involves generating a unique set of model output for a given set of input. The layer-cake model is used in modeling the Monument NW Field where each layer is divided into several grid blocks and into separate layers. Five layers were modeled in a total area of about 700 acres on average. A total of 2400 grid blocks were used to model the anticlinal reservoir structure. These gridblocks were now populated with values from well control values which was obtained from well logs and drill stem test. Using the fact that we have lateral and vertical heterogeneity some typical methods are used in populating the porosity and permeability values[13]. Also worth mentioning is the relative permeability tables which was developed using work from Byrnes and Bhattercharyna and drill stem tests.

Porosity Description

In assigning porosity value to each grid block, the porosity values derived from well log analysis are entered into the model on a well basis areally for each layer. Based on the areal trend the values are populated for a given layer. This population simply represents the pre-diagenetic porosity. The inverse distance method and the normal distribution methods were used for the five different layers. The inverse distance method populated layers with progressive increase or decrease in porosity values in a certain direction and the normal distribution method populated layers whose porosity values were par with the anticlinal structure of the layer. Figures 7 and 8 show layer maps of porosity after extrapolation. These initial grid populations will be distorted during the history matching phase.

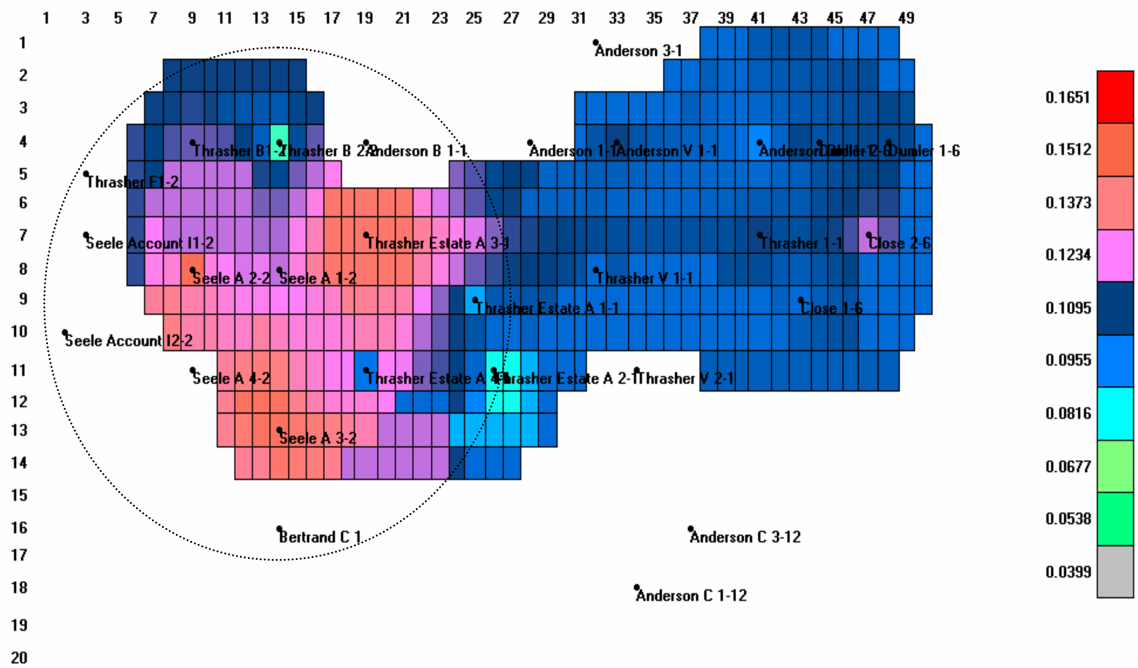

Figure 7: The Johnson layer porosity values. This was interpolated with a normal distribution method. The hatched circle shows the anticlinal porosity structure.

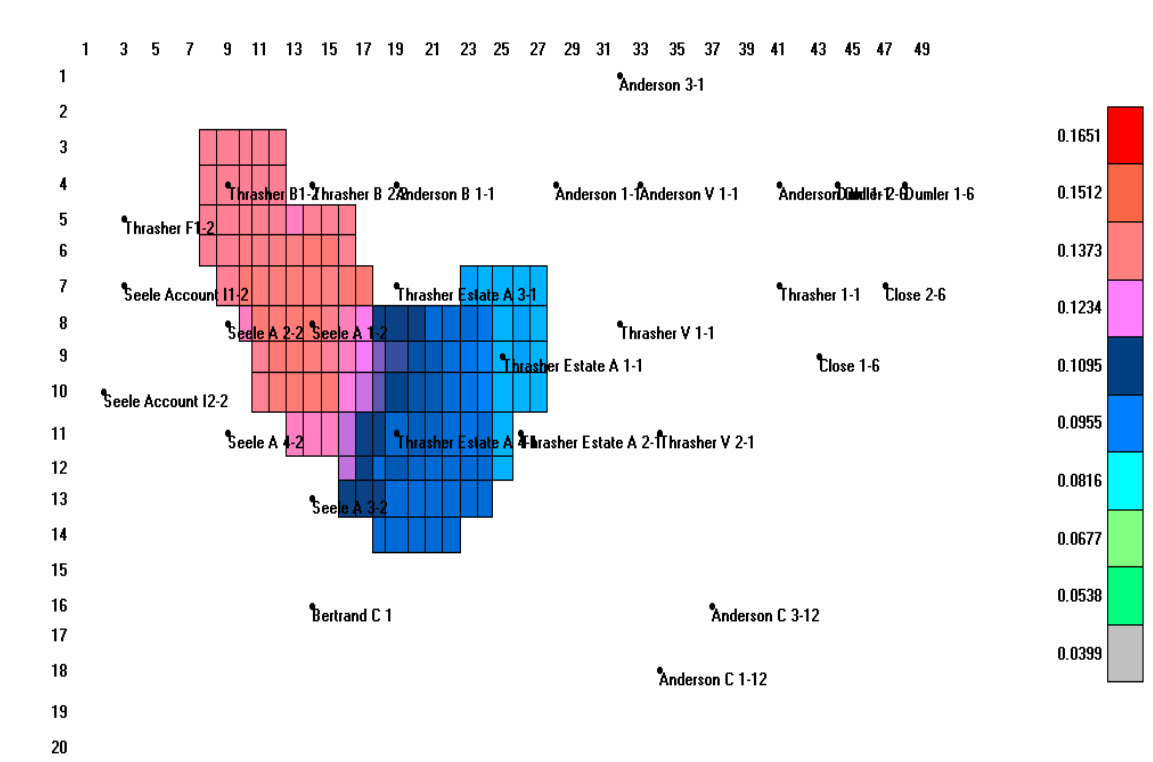

Figure 8: The H-Zone layer porosity values. This was interpolated with an inverse distance method.

Permeability Description

The permeability values were principally obtained from drillstem test analysis for each zone and this was populated using a logarithmic extrapolation. This method of extrapolation accounts for heterogeneity by covering a wider range of values. However, it must be noted that the derived extrapolated permeabilities are not final. These will be calibrated during the history-matching process to obtain a good match.

Relative Permeability

Byrnes and Bhattacharya studied the 950 cores from the Mississippian and Lansing-Kansing formation and defined a property called a trapping constant. The trapping constant is defined basically to relate porosity and residual saturations. For a given trapping characteristic, which is related to porosity, a relationship between the initial oil saturation and the residual oil saturation to waterflood is developed where the trapping constant, C, is defined as[5]

$$C = 1/S'_{or} - 1/S'_{oi} \tag{17}$$

where $S'_{orw} = S_{or}/(1 - S_{wirr})$ (18)

and $S'_{oi} = S_{oi}/(1 - S_{wirr})$ (19)

Byrnes and Bhattacharya approximated the land trapping characteristic as

$$C = 11.14\phi + 0.27 \quad \text{for } ø < 0.1 \text{ and} \tag{20}$$

$$C = 11.7\phi - 0.51 \quad \text{for } ø > 0.1 \tag{21}$$

and with these two equations, relative permeability tables are developed using the modified Brooks-Corey relative permeability equations.

$$k_{ro} = k_{romax}(1-S_{wD})^n \tag{22}$$

$$k_{rw} = k_{rwmax}S_{wD}^m \tag{23}$$

$$S_{wD} = (S_w - S_{wc})/(1 - S_{wc} - S_{orw}) \tag{24}$$

Two different relative permeability tables shown in Figures 9 and 10 were defined for two rock types. These two relative permeability curves had different propensity for water. The H-Zone and the K-Zone had a good propensity for water with the H-Zone having an aquifer. The I, J and Johnson zone had predominantly the same flow characteristics. The endpoints in equation 24 were satisfied iteratively from DST analysis and from the land trapping characteristic. Fluids produced during the drill stem test were analyzed to understand fluid flow characteristics for each zone. This was then tied against the permeability derived from the drill stem test analysis which basically give the permeability to oil.

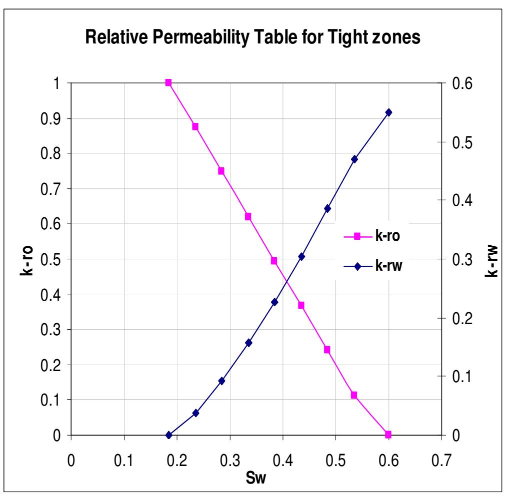

Figure 9: Relative permeability table for tight zones. This has a higher water propensity due to a higher capillary pressure of the non-wetting fluid.

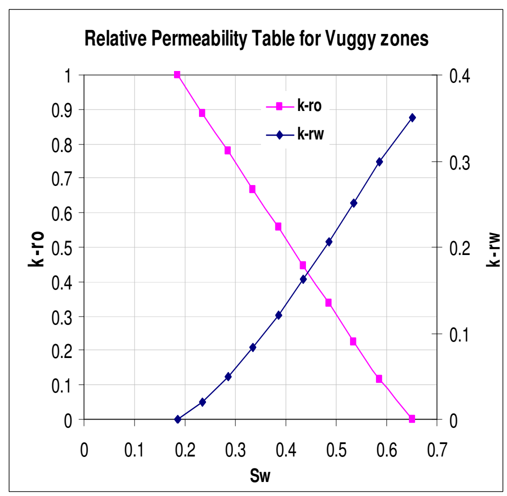

Figure 10: Relative permeability table for vuggy zones. This has a lower water propensity due to a lower capillary pressure of the non-wetting fluid.

Capillary Pressure and Initial Water Saturation

Initial water saturation is usually determined from capillary pressure entered into relative permeability tables[14]. This method creates a water distribution profile with depth. For the Monument Northwest field, the average net pay was about 5 ft. This does not leave room for a distribution profile without drastic changes. The initial water saturation for layers other than the H-Zone are assumed to be at or close to irreducible water saturation following geological history. To account for an initial water distribution in the H-Zone, a spatial relationship was developed that varied the water saturations laterally. The water saturation was distributed as a function of net pay height. This made the water saturation least at the top of the structure which had the highest net pay and the highest water saturation at the flanks were pinch-outs occur and aquifer starts. The H-Zone water saturation was defined in this manner and this helped increase the water production history match where the flank wells had higher water production. This ties in with the fluid migration history where water-in-place would settle due to buoyancy and migration direction. A linear relationship was developed as

$$S_w = S_{wc} + \frac{S_{w\max} - S_{wc}}{h_{\max} - h_{\min}}(h_{\max} - h) \tag{25}$$

Aquifer Definition

A Carter-Tracy aquifer was modeled at the top of the structure (H-Zone). This was done by influencing grid blocks on the west flank of the field. This aquifer is tied in with the migration and accumulation of the hydrocarbons which displaced formation water which was still trapped in the structure. The Carter-Tracy equation is given in finite difference form as[15]

$$W_e^{n+1} = W_e^n \frac{(F(p^0 - p^{n+1}) - W_e^n p_{t_D}^{n+1})(t_D^{n+1} - t_D^n)}{(p_{t_D}^{n+1} - t_D^n p_{t_D}^{n+1})} \tag{26}$$

Where F is a constant and p_{tD} is the pressure influence function at t_D. For a finite aquifer this is proportional to the natural logarithm of r_a/r_w. After defining the aquifer, we used a horizontal influx function (using face x-z and y-z of west flank grid blocks) for aquifer fluid displacement.

It should be noted that the aquifer modeled was not modeled in the initial model development but during the history matching phase of the project. It is done this way to know how to calibrate and model the aquifer as a finite aquifer by checking the pressure offsets in the layer pressure match for the H-Zone. More so, other aquifer data such as the aquifer permeability was calibrated by the water production match from the wells producing in the H-Zone.

Model Initialization and History Matching

After the model is built and production data is loaded, it is time to initialize the model. This is simply verifying the volumetric and physical model. To do this, we run the simulator model for an infinitesimal time step[16]. This is a way of making the simulator to check if all the parameters are mathematically stable for a next forward approximation. The oil-in-place is an important parameter obtained from this process and this is compared to the evaluation from the geologist. For the Monument NW field, the isopach maps used for the model development were made by the geologist so this made it easy to get a match on oil-in-place at the first go. Table 5 shows a summary of the model initialization.

Table 5: Model initialization results after isopach alterations.

Pore Volume, MBBL	**3863**	**2985**
Stock Tank Oil, MMstb	**2.723**	**1.89**
Total Gas, Mcf	**0.137E+06**	**0.263E+05**
Free Gas, Mcf	**0**	**0**
Water, MMstb	**1.3**	**0.9062**

These values differ from the geologist values as two wells Anderson C#1 and Anderson C#3 are modeled in the reservoir model by extending the isopach maps in certain layers. A reservoir simulator equations use pressures at the center of the gridblocks. These pressures represent material balance average pressures in the gridblocks using the diffusivity equation as the flow condition for displacing the oil and gas under a finite difference scheme. The diffusivity equation is simply a combination of the equation of state, the continuity equation and conservation principle. This is simply given as[17] (in global space)

$$\nabla^2 p = \alpha \frac{\partial p}{\partial t} \tag{27}$$

and can be discretized in a one-dimensional cartesian coordinate as[17]

$$\frac{p_{i-1}^{n+1} - 2\,p_{i}^{n+1} + p_{i+1}^{n+1}}{(\Delta x)^2} = \frac{\phi\mu c}{0.00633\,k}\,\frac{p_{i}^{n+1} - p_{i}^{n}}{\Delta t} \tag{28}$$

For gridblocks holding wells, additional equations are used to relate well performance to cell variables. Assuming steady state flow occurs within a cell, flow equations are given as[14]:

$$q_o = J_{model}\left(\frac{k_r}{B\mu}\right)_o^n (p_{i,j}^{n+1} - p_{wf}) \tag{29}$$

$$q_w = J_{model}\left(\frac{k_r}{B\mu}\right)_w^n (p_{i,j}^{n+1} - p_{wf}) \tag{30}$$

$$q_g = J_{model}\left(\frac{k_r}{B\mu}\right)_g^n (p_{i,j}^{n+1} - p_{wf}) + Rs^{n+1} q_o \tag{31}$$

Where J_{model} is the well index given by Peaceman as[17]

$$J_{model} = \frac{2\pi(0.00633)kh}{\ln r_o / r_w + s} \tag{32}$$

And r_o is calculated based on permeability anisotropy. Equations 29-31 present three equations with four unknowns: q_o, q_w, q_g and p_{wf}. This implies that for a simulator run, the user must specify one of these unknowns and the simulator will produce the well[17]. After the well is produced, we can compare simulator performance with actual data if available. This is a vital step in simulation as this helps to reduce uncertainty of the simulator model. This is called reservoir history matching.

History-matching is the process of calibrating the reservoir model so that the simulator results closely follows or is the same as the observed data. Production data and pressure are measurements used during this phase. Typically for a reservoir simulator run, either the fluid rate is specified or a pressure constraint is used to satisfy the material balance[16].

We used the fluid withdrawal constraint for this project. This scheme uses production data which was measured and recorded as a simulator input. The fluid was then withdrawn, and a pressure match was obtained. A total of 11 wells and 5 zones would be matched. To do this, we constructed a flow diagram that assisted us in the history matching process. This was done in a chronological manner by well completion time history following a zone-zone basis. After covering a reasonable acreage, the match is continued on a proximity basis. The chart shown in Figure 11 gives an idea on how to calibrate reservoir properties for obtaining a match with less iteration.

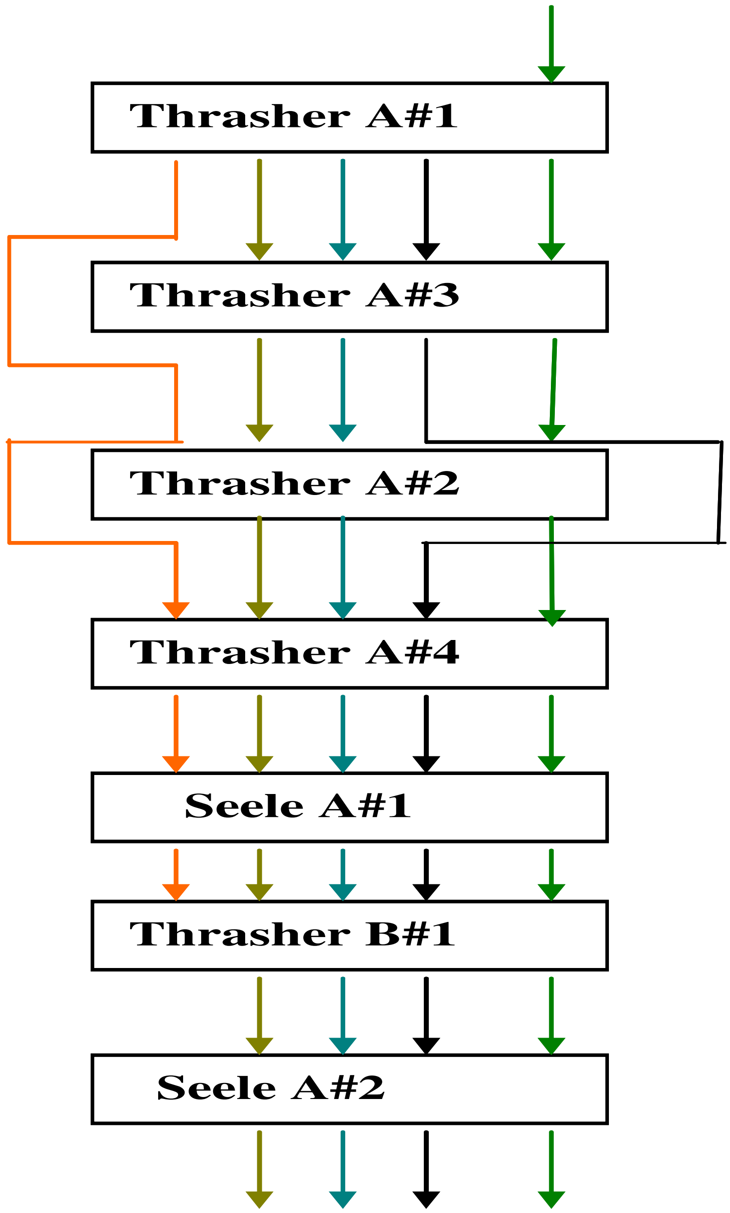

Figure 11: Chronological chart of the first seven completed wells. Different colors of arrow represent different zones, and going into a well represents a completion of the well in that zone.

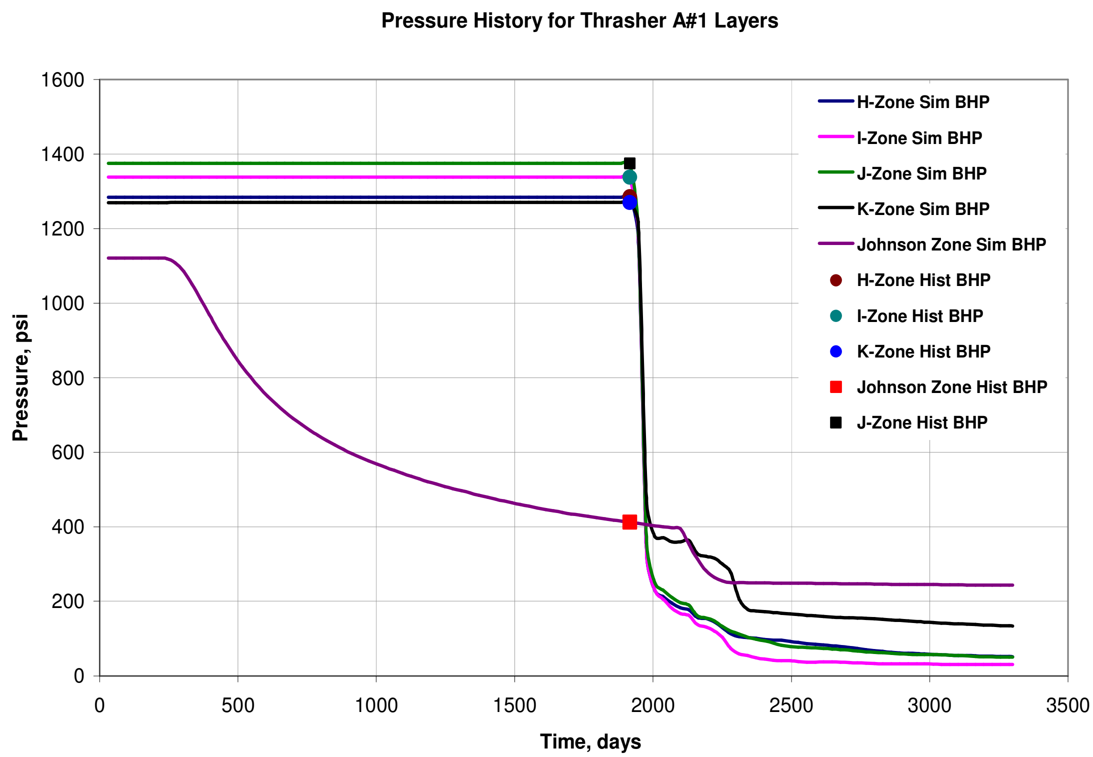

Figure 12: Pressure match for layers in the Thrasher A#1 well.

Thrasher A#1 match (see Figures 12 and 13) was easily obtained since it is the first well drilled into the top four layers. The Johnson zone is an extensive structure and extends beyond the Monument Northwest acreage. Some wells were modeled into the Johnson zone to begin production from 03/01/1997 which is the date that production commenced from that structure. The flat line before the decline is for model initialization, this is between 01/01/1997 and 03/01/1997. No production well is turned on at this time. In as much as the pressure history match for Thrasher A#1 is easily obtained, we still have to match the well production history. The well production history is a match of fluid produced from the well and a corresponding match of both the well historical static bottom-hole pressure and the flowing bottom hole pressure. The Thrasher A#1 well was put on a pumping unit within months of production, therefore we expect to see a minimal flowing bottom hole pressure as shown below:

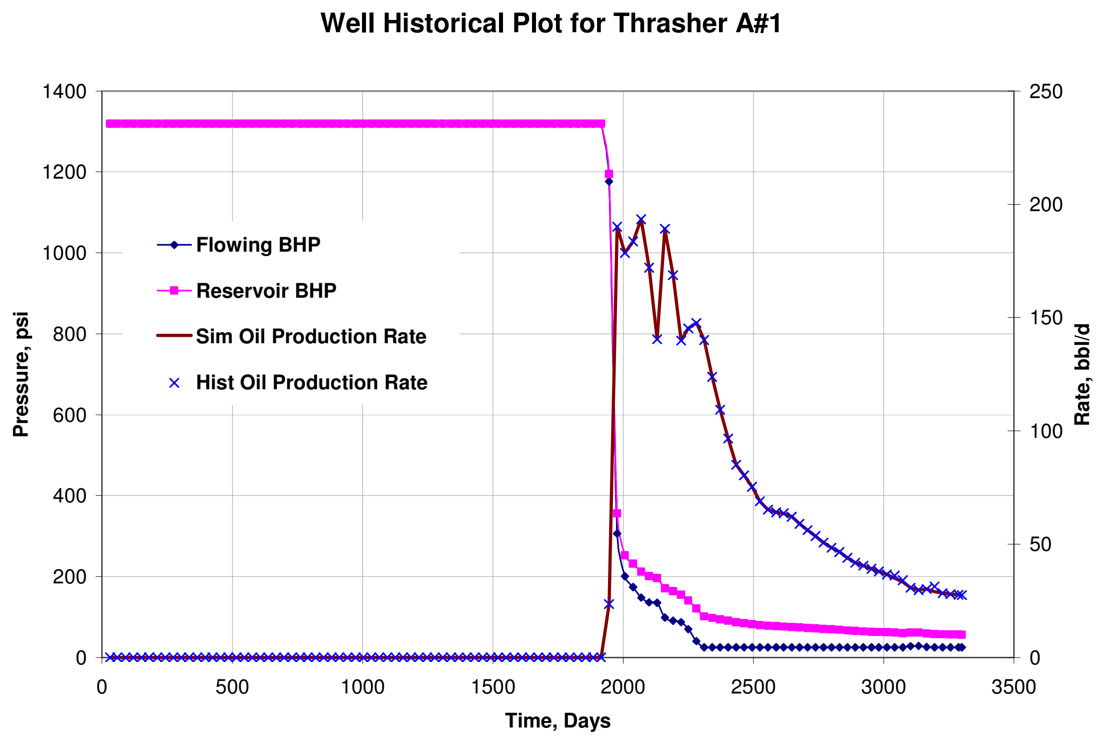

Figure 13: Well historical plot for Thrasher A#1. This shows the bottom-hole pressure reducing with production and the well pumped off.

The layer pressure match is first obtained for all wells before a single well production history match is made. This was achieved by specifying a total reservoir fluid volume (oil and water) constraint to first match the layer pressures. This ensured that the fluid actually produced from the reservoir can actually be matched. The constraint was then reverted back to an oil-rate constraint for which a well production history match was made followed finally by a fluid match on a well basis. This is shown with a flow chart in Figure 14:

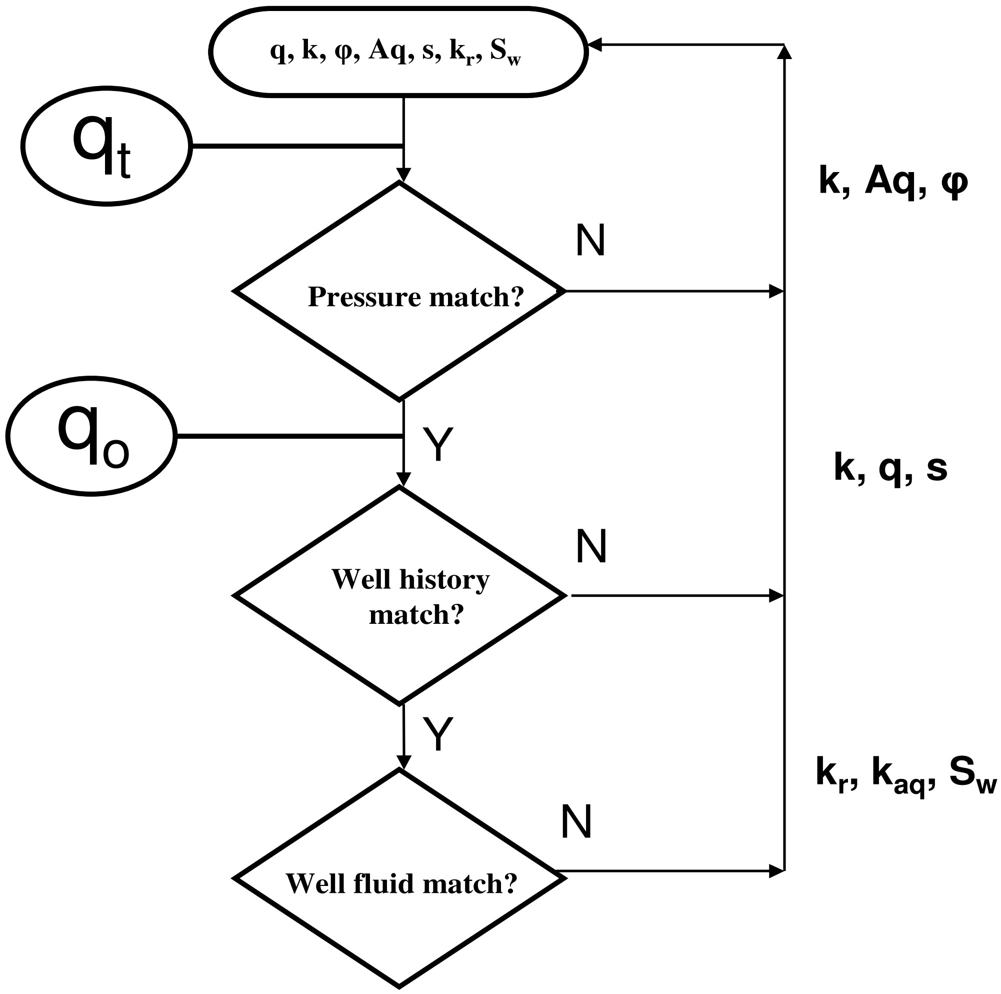

Figure 14: Flow diagram for history matching process used. Decision 2 usually throws off automatic history matching schemes.

There are an infinite number of models which will give equally reasonably matches of data so it is desirable to define a procedure for generating a particular estimate or to characterize the uncertainty in the reservoir description[6]. This is where manual history matching methods supersedes automatic history matching methods. Automatic history matching involves the minimization of an objective function which is commonly expressed as[18]

$$O(m) = (g(m) - d_{obs})^T Cov_d^{-1} (g(m) - d_{obs}) \tag{33}$$

Where d_{obs} represents the observed production data, g(m) represents the production data predicted by the simulator as a function of a model parameter m. To minimize the objective function usually needs the gradient of the objective function to be taken and this often requires the computation of a sensitivity matrix which involves the relation between the model parameter and the data. This would be fast and easy for a system that simply involves a pressure match by changing permeability.

The Monument Northwest field has two factors that limit the workability of automatic history matching methods: one of the zones has an aquifer, and each well was put on a pumping unit at an average time of 100 days after initial production –this is an equivalent to specifying a flowing bottom-hole pressure. Some rigorous history matching simulator could work with the first limit by assigning a weighting factor to the aquifer model and use this as a column vector in the sensitivity matrix. However, it is virtually impossible to work automatically with the second constraint. This would imply imposing a double standard on the simulator.

Inasmuch as the second constraint is ambiguous, it helps improve our model with respect to the history matching process. Actually, this was one of the biggest advantages of manual history matching methods with respect to this project. The reservoir engineer now knows every corner of the reservoir and a better knowledge and reservoir characterization of the reservoir is achieved. For example, after tweaking permeability within a reasonable range and a well production history match is not achievable in the simulator, we can infer that the actual well must be damaged and that was why it required a pumping unit early in the life of a well. So to achieve the historical event of the pumping unit, we now add a skin to the well which now facilitates the excessive pressure drop at the well. Such well would be tagged as a stimulation candidate particularly if the production rate drops from a usual trend.

Figures 15-17 show the match for Thrasher A#4 well which went under production 8 months after Thrasher A#1:

Figure 15: Pressure match for Thrasher A#4 well at 01/06/2003. H-Zone pressure kept high by aquifer.

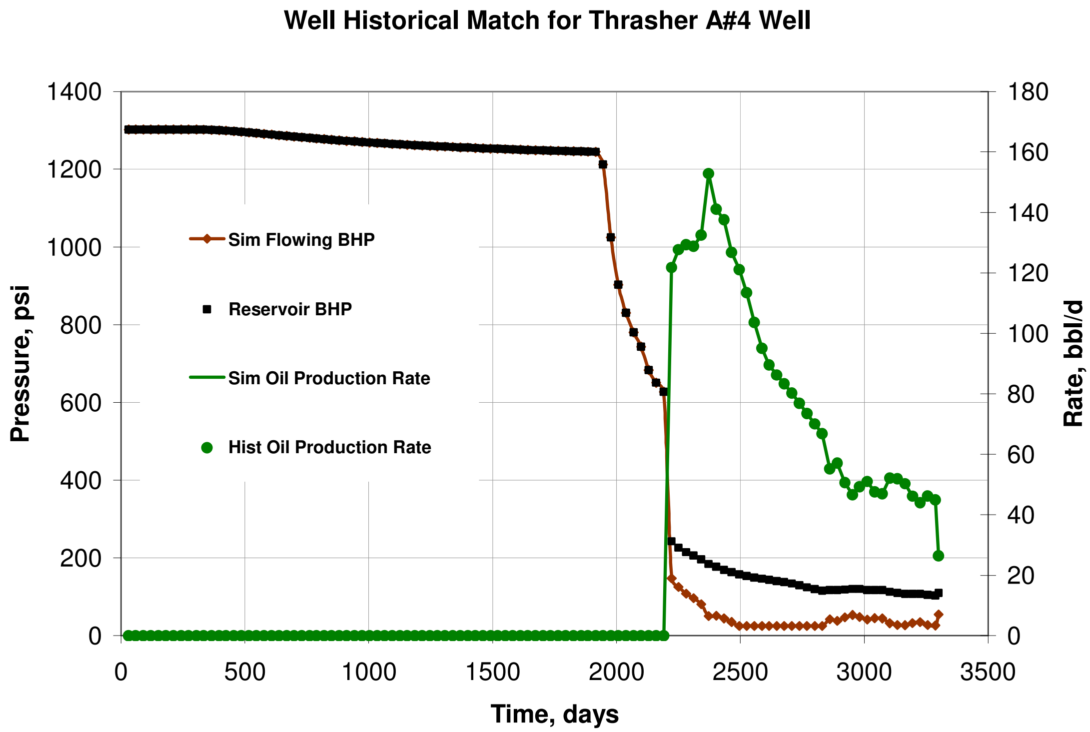

Figure 16: Historical well match for Thrasher A#4. This well is also pumped off shortly after production.

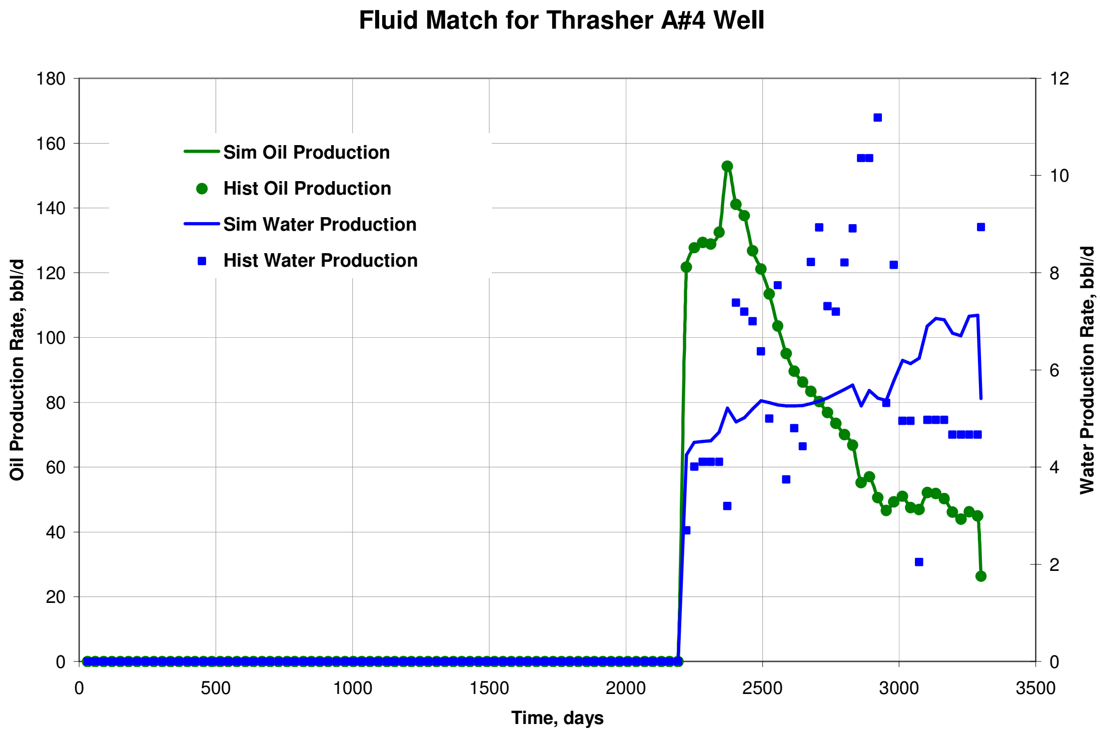

Figure 17: Fluid match for Thrasher A#4 well. The water production does not necessarily match but the trend is followed.

It is important to note at this point that a 100% match is not necessarily achievable[6,18]. The most important thing is maintaining reality at all times. And also, a well fluid match may not be 100% precise because the actual cases measured production data in leases which were allocated to individual wells in the simulator using theoretical decline methods which are at best, estimates of actual well production data. The exponential decline was used in splitting up lease data into well data and forecasting.

CHAPTER V

WATERFLOODING MONUMENT NW FIELD

Simulating a waterflood was the objective of the overall study. Now that we have a replica of the reservoir we simulate a waterflood recovery by injection. A few factors should be considered and analyzed before a waterflood[19]. For the Monument Northwest field these included:

- Selection of injection wells
- Fracture gradient of the formation
- Proposed injection rate and cumulative injection volume for a full sweep
- Conversion costs of well
- Gravitational and discretization effects

Layer Subdivision

Before discussing the details of the waterflood, it is important to explain the discretization and gravitational effects of a water injection with respect to the displacement in the grid block. When there is an influx of saturation on a grid block, the simulator implicitly satisfies material balance for that grid block by displacing inherent saturations and increasing the grid block pressure. The simulator also tries to satisfy the gravitational effects of the different saturations. This can lead to numerical dispersion which is a common problem with simulators. Numerical dispersion simply means a blow-up of discretization errors. We helped minimize this problem in this project using layer subdivision prior to injection. We simply divided a layer into three equal compartments with same properties. The idea behind this is that if you inject into H-Zone, which is now in three layers, water will preferentially fill the lowest layer. This helped reduce the dispersion problems while at the same time simulating reality.

Selection of Injection Wells

This was not a simple straight-forward task as this involved zones that are all of different area, shape and with different number of wells. As usual, we tried using our constraints as leverages in our analysis. Using the constraints, we tried optimizing areal sweep efficiency and minimizing water breakthrough time for producer wells while checking that actual injection rates can be achieved with the stated fracture gradient bearing in mind that the areal sweep efficiency of a waterflood before breakthrough is directly proportional to the recovery[19].

The injection rate is proportional to the injection pressure and the injection pressure should be less than the fracture pressure hence a fracture would occur[19,20]. The fracture pressure is simply the fracture gradient multiplied by the corresponding depth. Therefore to achieve good injection rates without back-pressure or fracturing, the reservoir permeability should be favorable. The injection rate and injection pressure are given by Darcy's law as[10,19]

$$i_w = \frac{0.00708\,\bar{k}\,h_t\,(p_{wf} - \bar{p})}{\mu_o \ln(r_e / r_w)} \tag{34}$$

where $\bar{k}$ is the average combined layer permeability calculated as

$$\bar{k} = \frac{k_1 h_1 + k_2 h_2 + k_3 h_3 + k_4 h_4 + k_5 h_5}{h_t} \tag{35}$$

From equation 34, we observe that to inject below the fracture pressure, the reservoir pressure and the permeability play the most important. From the fact that we have lateral heterogeneity in the reservoir, we used the radial permeability of the grid block holding the well for the computation of equation 35. This assumes that the grid blocks holding the well transmits the water and should a fracture occur, it should start from the well[20,21]. A field injection rate constraint of 1000 bbl/d was used together with a maximum injection pressure of 2500 psi for each well. This maximum injection pressure was justified using a fracture gradient of 0.7 psi/ft with a safety gradient of 0.1 psi/ft. This upper limit watched the window because to inject at the constant injection rate, the injection pressure will increase due to increased reservoir pressure. Therefore there comes a time when the injection rate may be reduced to satisfy the maximum injection pressure constraint or the simulator will quit in error. This is observed from the simulated injection wells' profile (see Figures 18 and 19) where the flowing bottomhole pressure and the injection rate for the injector well is plotted together against time.

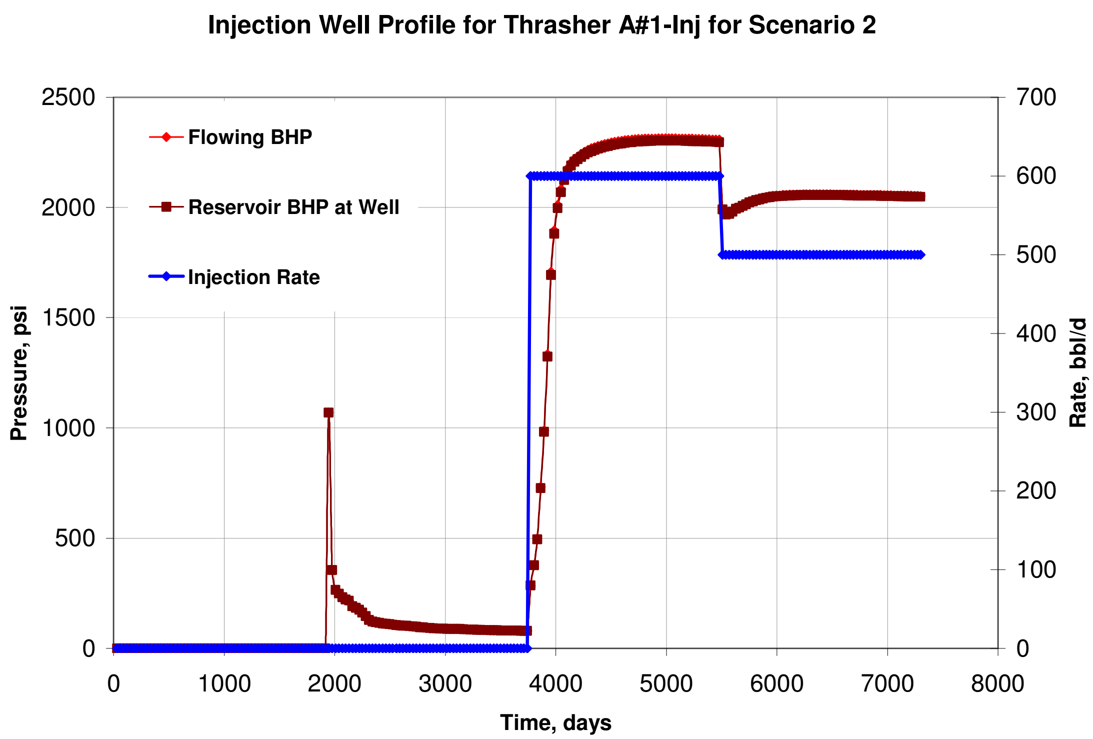

Figure 18: Injection well profile for the Thrasher A#1 injection well. At 5478 days, rate was changed to stop pressure build-up in injector and also to increase rate for other injector well Seele A#1 for the optimum case.

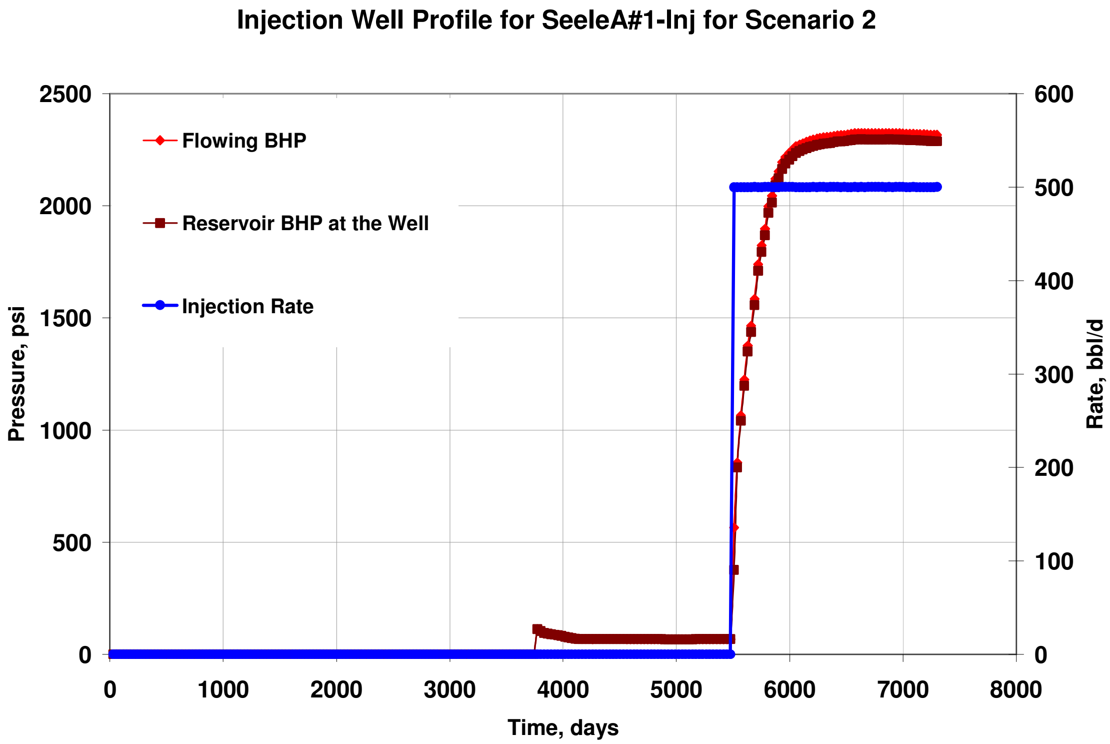

Figure 19: Injection well profile for Seele A#1 injector well. Injection in this well commenced at 5478 days at 500 bbl/d while injection was taking place at Thrasher A#1-Inj simultaneously.

Waterflood Scenarios

Five waterflood scenarios were modeled and compared against a do-nothing case. The Monument Northwest field proved to be in need of a waterflood project as all scenarios presented improved economics of the field against the base case which is termed the "do-nothing" scenario.

Table 6 below shows a brief description of the different scenarios

Table 6: Showing the various waterflood scenarios simulated. An attempt to improve field economics for the Monument Northwest field was made.

Scenario #	Injector Wells	Date Effective	Injection rate, bbl/d
1	**N/A**	**N/A**	**N/A**
2	**Thrasher A#1-Inj** **Seele A#1-Inj**	**08/01/2007 |01/01/12** **01/01/2012**	**600 | 500** **500**
3	**Thrasher A#1-Inj** **Seele A#1-Inj**	**08/01/2007 |01/01/12** **08/01/2007**	**600 | 500** **400**
4	**Thrasher A#1-Inj** **Thrasher B#1-Inj**	**08/01/2007 |01/01/11** **08/01/2007**	**600 | 500** **400**
5	**Thrasher A#1-Inj** **Thrasher B#2-Inj**	**08/01/2007 |01/01/11** **08/01/2007**	**600 | 500** **400**

Scenario 2 proved to be the best case in terms of economics. Pressure support is maintained by injecting in Thrasher A#1-Inj and production is kept high from the other ten producing wells. However after about 2000 days after the start of injection, an areal sweep is achieved (as shown in Figure 20) to an extent where converting Seele A#1 to an injector as well becomes the best option for the field as the well now has water breakthrough and would further enhance the areal sweep to other parts of the field. Shown in Figures 21-23 are field-wide production details for the different scenarios.

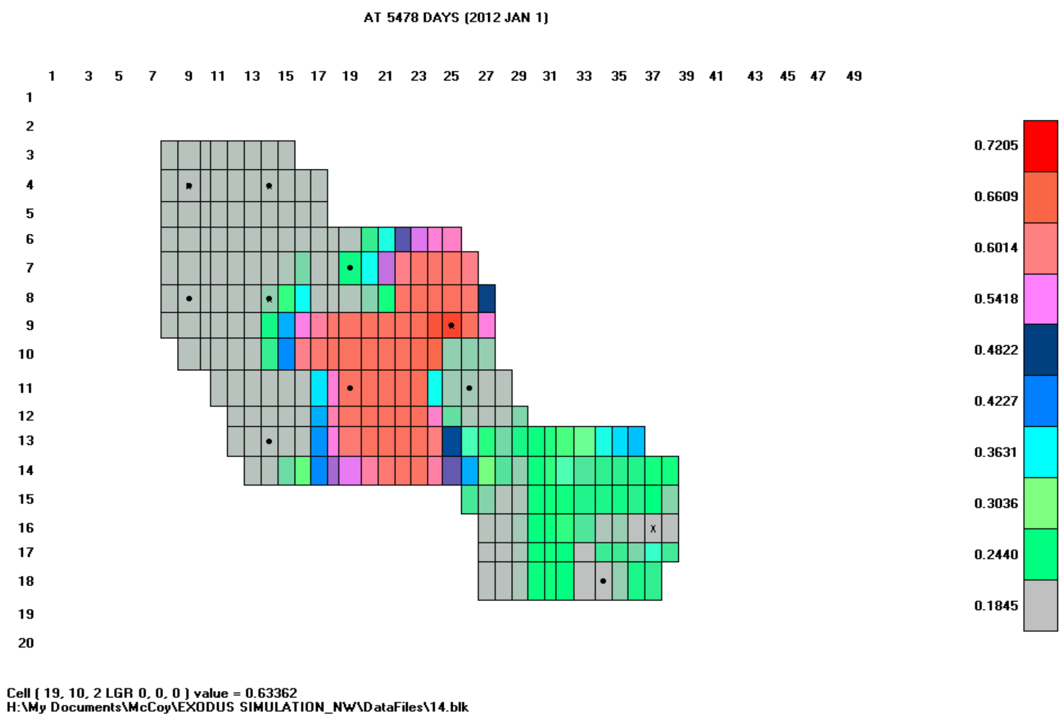

Figure 20: Water saturation map at 5478 days. The areal sweep for this layer up to Seele A#1 is good and to keep up production from other unswept areas Seele A#1 is made an injector at this time.

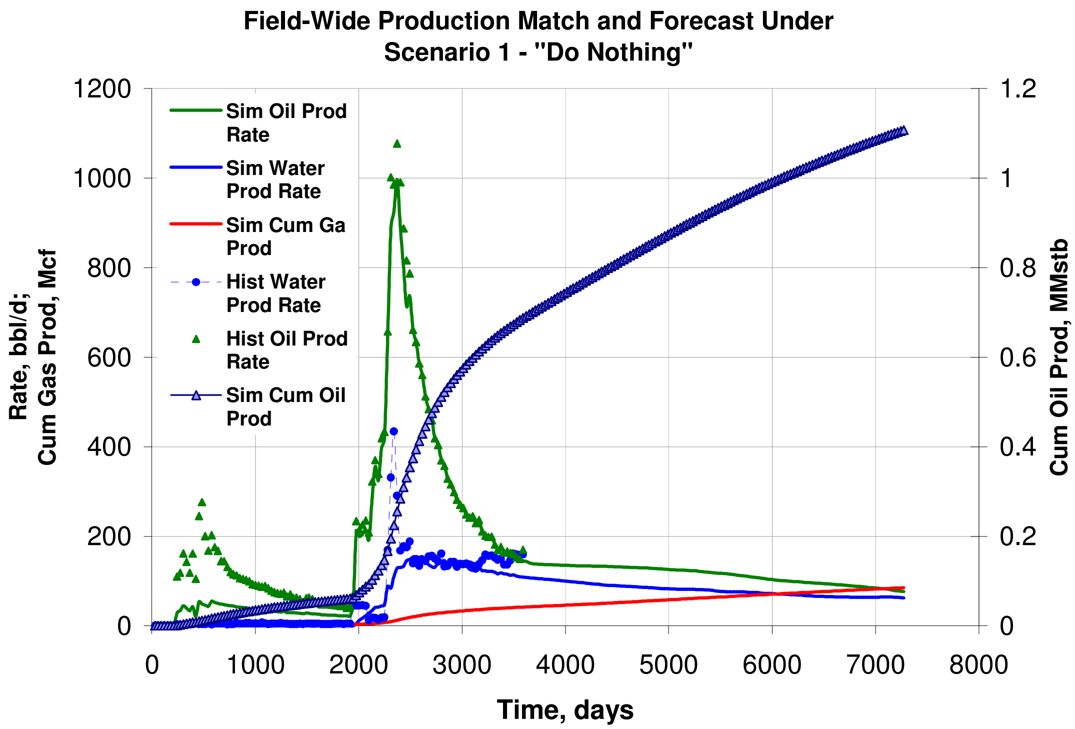

Figure 21: Field-wide production details for scenario 1. Scenario 1 waterflood scheme is basically just continuing production without any waterflood.

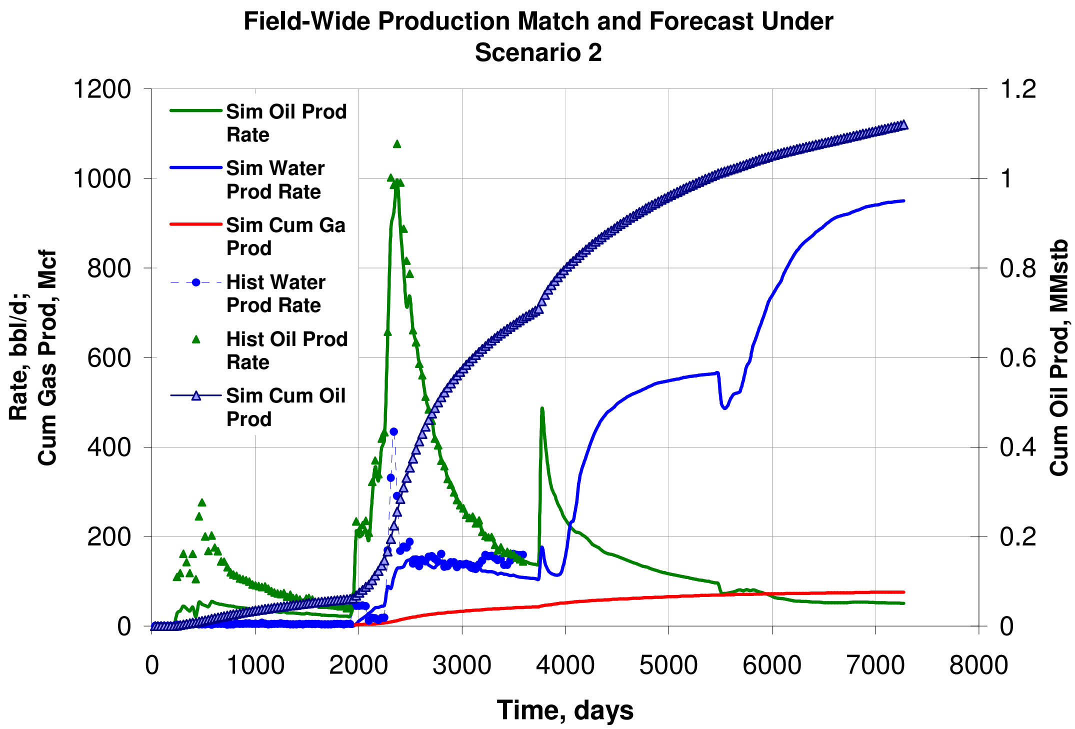

Figure 22: Field-wide production details for scenario 2 waterflood scheme. We have high production performance of oil and water. The water is simply re-injected. At 5478 days we have two injectors keeping the field production from declining fast.

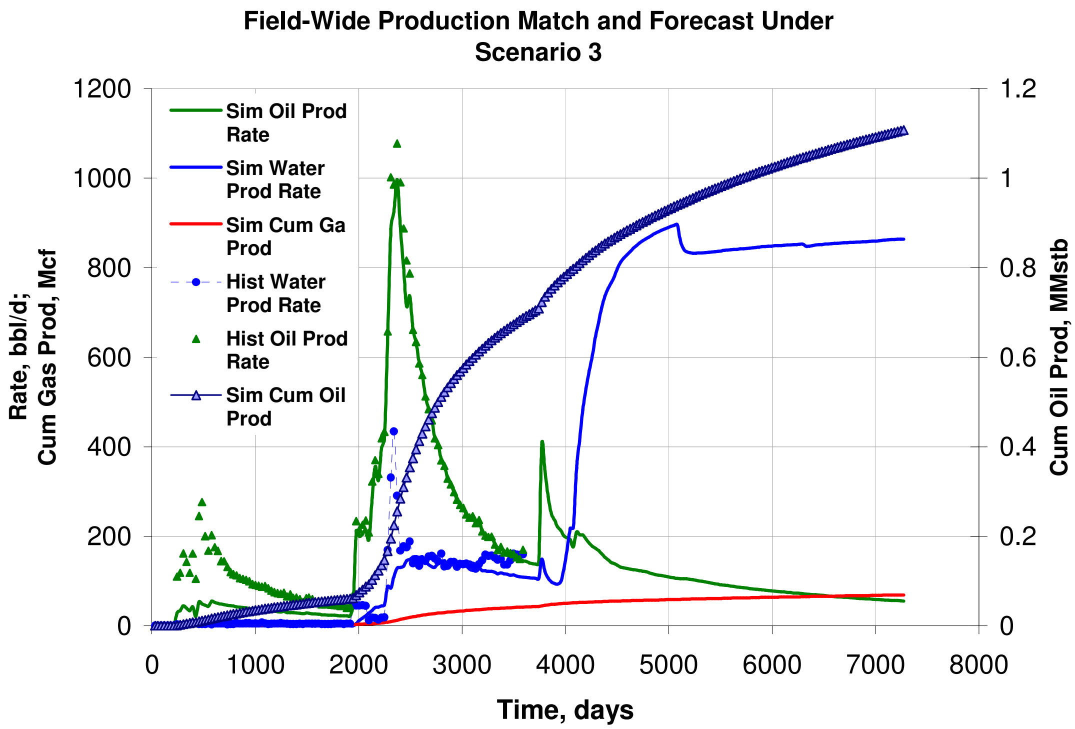

Figure 23: Field-wide production details for scenario 3 waterflood scheme. This is similar to Scenario 2 but we used two injectors right from the start of the waterflood. This scenario proves that the idea of converting Seele A#1 well to an injector later in the project is a good one.

Project Evaluation

For the economics runs (see Figures 24 and 25), statistical parameters used for the economic evaluation are as follows:

Conversion cost per well: $50,000

Saltwater handling facility: $100,000

Oil price: $60/barrel

Gas price: $7/Mcf

Operating costs: $2,500/well/month

Royalties: 18%, 8% overriding royalty

Discount rate: 10% per annum

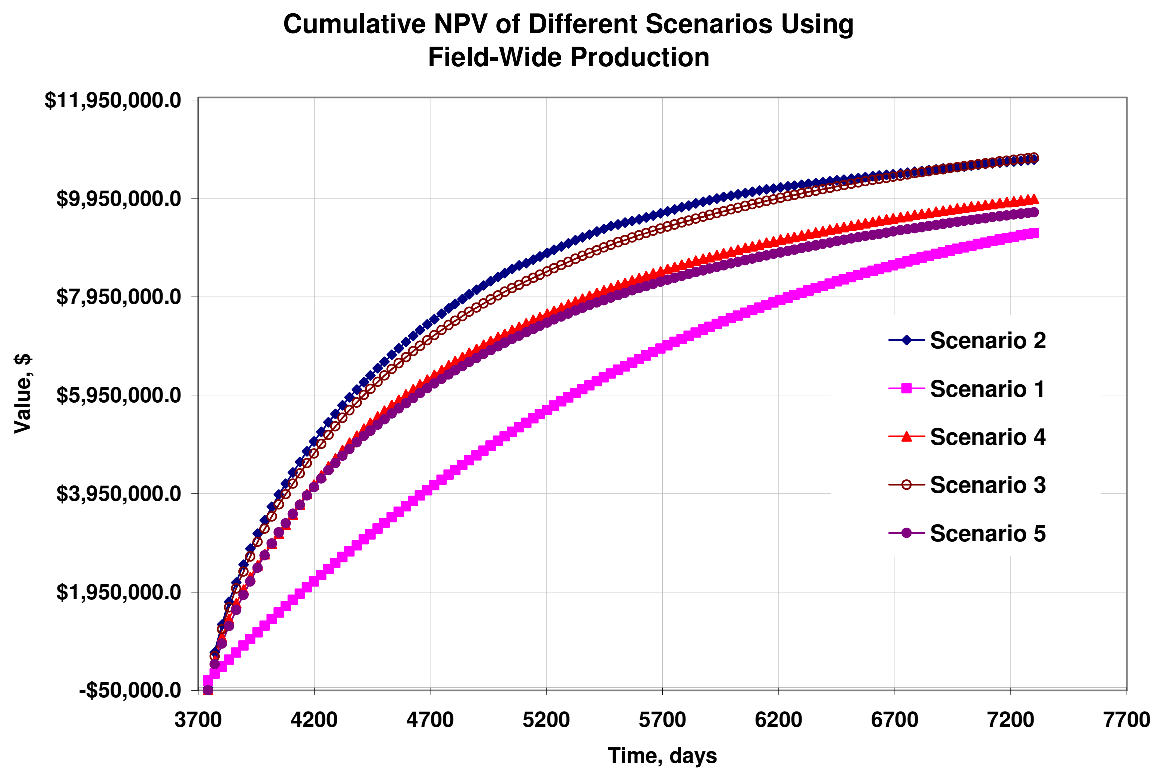

Figure 24: Cumulative NPV of the different waterflood scenarios. Scenario 2 represents our best case scenario.

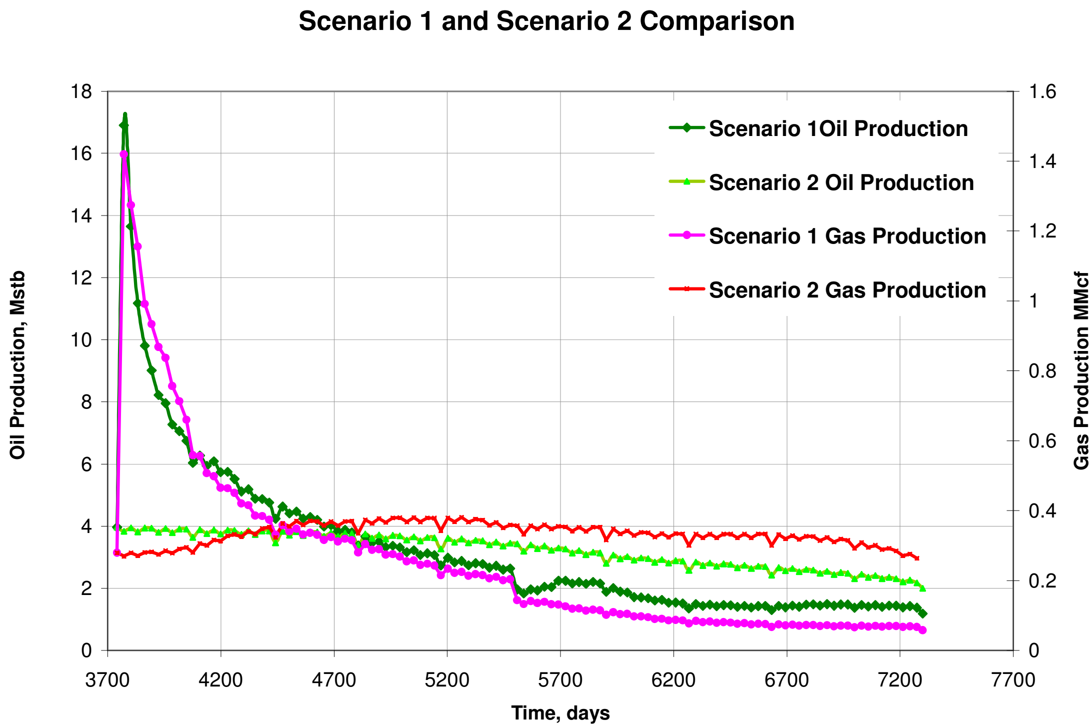

Figure 25: Production profiles of scenario 1 and scenario 2. The scenario 1 immediately increased oil production but declined quickly due to water breakthrough in producing wells.

Monte Carlo Analysis

Deterministic methods of evaluation were used during the course of this project. However, it must be emphasize that model results are probable since there are a possible different models that can match our historical data which everything seems to be based off from[6]. A stochastic approach is used in the economics to associate probabilities with values so the operator or investor can have certain expectations and risk evaluations.

Monte Carlo algorithm is an evaluation technique where a group of parameters are being used in an analysis in a stochastic manner. Pseudo-random numbers are generated for certain parameters whose values fall in within a range given by a certain distribution. Figure 26 shows the triangular distribution which was used. This analysis was applied on Scenario 1 by varying the oil price, the gas price, and the discount rate using a triangular distribution.

The triangular distribution is mostly used in business decision-making when the distribution has no certain pattern but one can confidently guess the mode, c, an upper limit, a, and a lower limit, b. This is given by

$$f(x \mid a,b,c) = \begin{cases} \dfrac{2(x-a)}{(b-a)(c-a)} & a \leq x \leq c \\ \dfrac{2(b-x)}{(b-a)(c-a)} & c \leq x \leq b \end{cases} \tag{36}$$

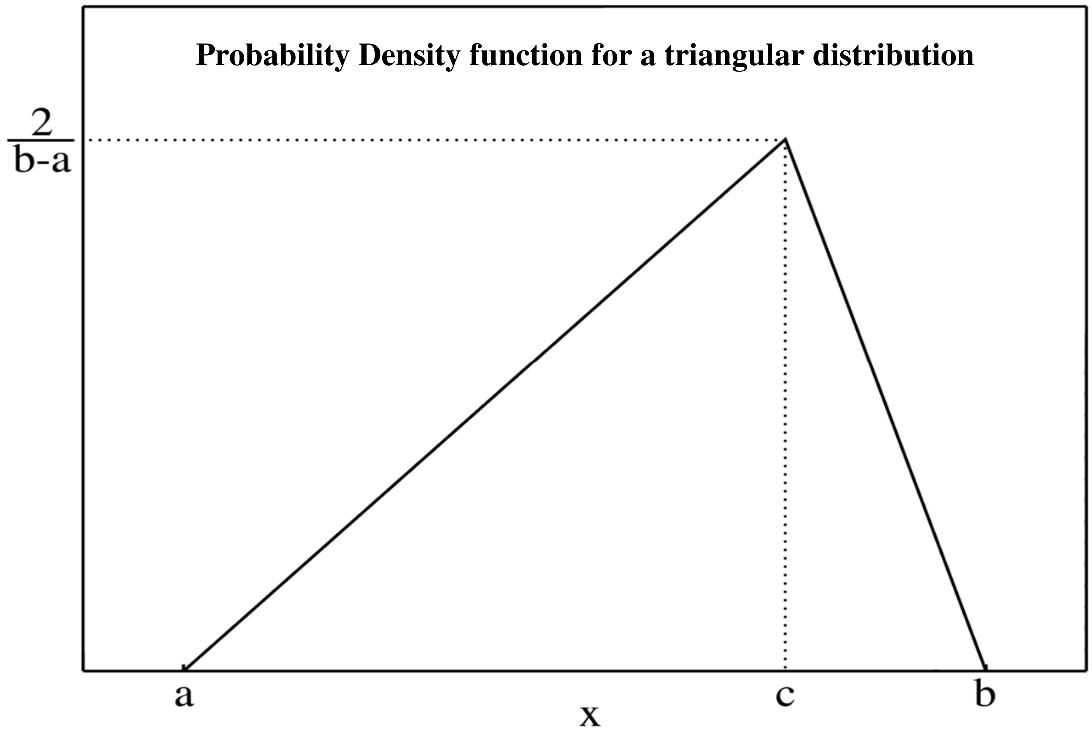

Figure 26: A typical triangular distribution curve

Table 7 below shows the values used as the limits and modes for the triangular distribution of the parameters varied in the Monte Carlo analysis.

Table 7: Economic parameters varied in the Monte Carlo analysis

parameters limits	Oil price, $	Gas price, $	Discount rate
a	45	4	0.06
b	65	7	0.10
c	90	10	0.125

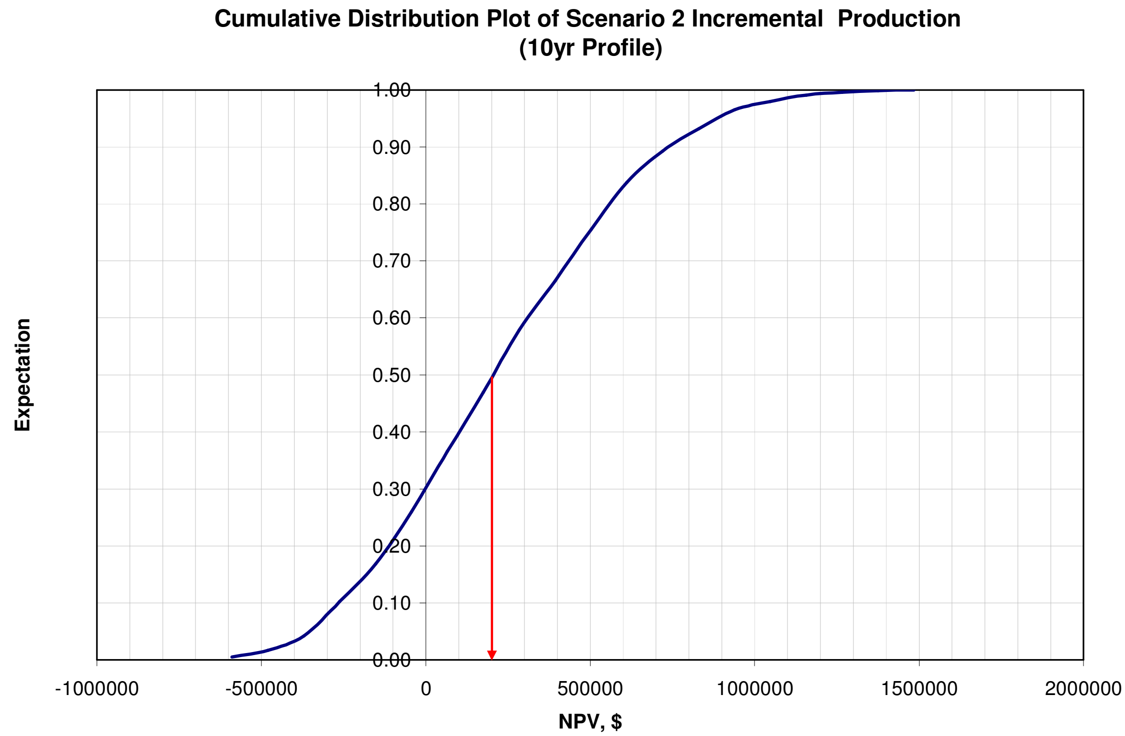

Figure 27: NPV plot incremental production using a 10-year production profile. This shows an expectation of $200,000 profit as compared to doing nothing. This is because the advantage of the waterflooding is experienced in the first 3 yrs after which the production is less than the "do nothing" scenario.

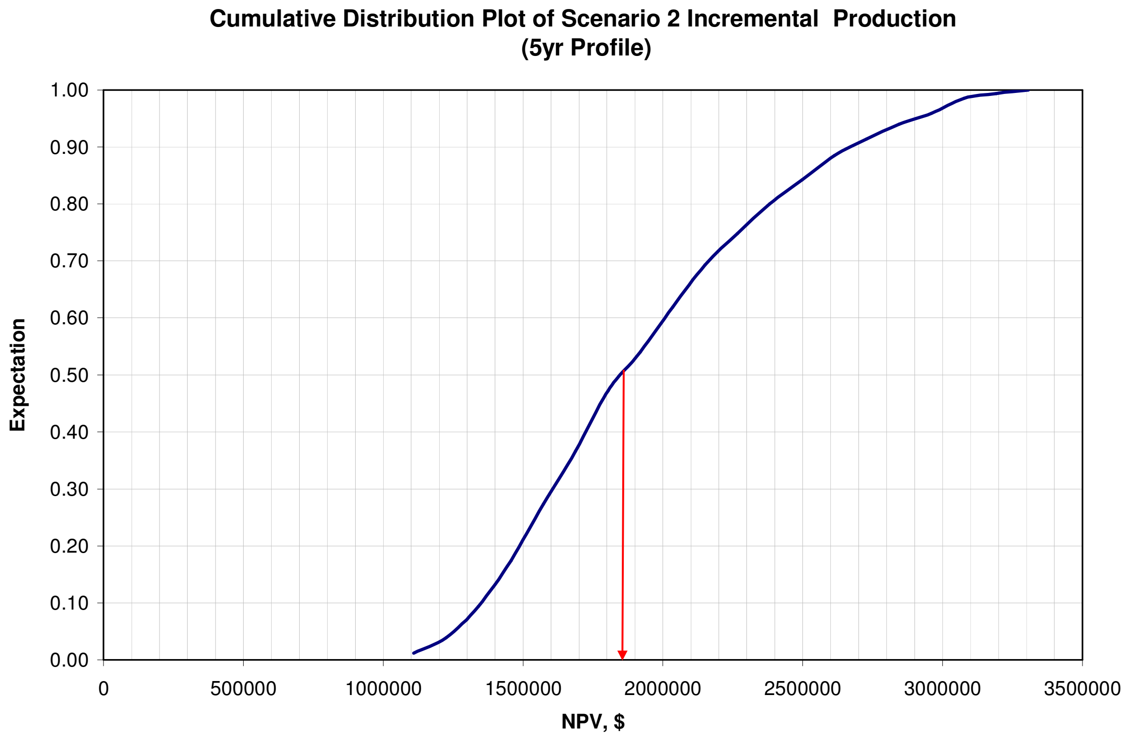

Figure 28: NPV plot of incremental production using a 5-year production profile. This time we expect a value of $1.9 million from the project. This looks more profitable because more of the time analyzed had the waterflood case doing much better than the "do nothing" case. This also says that the minimum profit in the short run from the project is $1.1 million.

Conclusions and Recommendations

Understanding the geology of the Monument Field NW area is a key in the evaluation and development of a deterministic model. Consistency and intersection of information from different segments was achieved with good confidence. Manual methods of history matching help build the confidence as constraints not usual for the simulator under automatic methods are being used to further define the well and reservoir properties for a better match or in some special cases a diagnosis of the well could be obtained.

Waterflooding the Monument Northwest field is a viable option to improve the economics of the field. The waterflood increases the field recovery by about 6% but the improved economics is more a function of accelerated returns than of increased recovery. The water injection increases the reservoir pressure and the performance is improved momentarily until water breaks through in adjacent wells. Once water has broken through, not much unswept oil can be recovered. This poses a problem for enhancing ultimate recovery.

A Monte-Carlo analysis was used to evaluate results from different scenarios so the time-worth and the risk of the project could be analysed. This can be seen in Figures 27 and 28. The analysis produces different results depending on the span of the project analyzed. Results have shown that analyzing a short span of the waterflood project presents attractive economics due to the fact that initial periods after the start of injection has higher production performances hence better cash flow than the case of no water injection. However, the results of a much longer time frame of the project diminishes the attractiveness of the economics because during the later part of the time frame analyzed, the case of no injection still has oil through-put at low cost while the initial aggressive performance of the waterflood project has been damped due to water breakthrough. Overall, it is still on the positive side of the economics and this makes the waterflood project viable on different fronts.

NOMENCLATURE

Aq	aquifer
c	compressibility
C	wellbore storage coefficient
Cov	covariance matrix
GR	gamma ray
H	thickness
k	permeability
p	pressure
PHIA	absolute porosity
PHID	density porosity
PHIE	effective porosity
PHIN	neutron porosity
q	rate
r	radius
R	resistivity
Rs	solution gas-oil ratio
s	skin
S	saturation
t	time

Symbols

Δt	time step size
Δx	gridblock size
ϕ	porosity
μ	viscosity

Subscripts

cln	clean formation
D	dimensionless
f	flowing
i	initial, counter
o	oil
w	water, well
s	static
shl	shaly formation
t	true

REFERENCES

1. North, F.K.1985. *Petroleum Geology*, Boston: Allen Unwin.
2. Dunham, R. J. and Folk, R. L.1962. Classification of Carbonate Rocks According to Depositional Texture. In *Classification of Carbonate Rocks,* ed. W.E. Ham, Chap. 2, 6-9. AAPG Memoir 1. Tulsa: American Association of Petroleum Geologists.
3. Foster, N. and Beaumont, E.1990. *Formation Evaluation II: Log Interpretation*, AAPG Reprint Series, AAPG, Tulsa **17:** 69-71.
4. Ahr, W.M. 2007. Carbonate Reservoir Geology Class notes, Texas A&M University, College Station.
5. Byrnes, A.P. and Bhattacharya, S. 2006. Influence of Initial and Residual Oil Saturation and Relative Permeability on Recovery from Transition Zone Reservoirs in Shallow Shelf Carbonates. Paper SPE 99736 presented at the 2006 SPE/DOE Symposium on Improved Oil Recovery, Tulsa, Oklahoma, 22-26 April.
6. Rietz, D. and Usmani, A. 2005. Reservoir Simulation and Reserves Classifications -Guidelines for Reviewing Model History Matches to Help Bridge the Gap Between Evaluators and Simulation Specialists. Paper SPE 96410 presented at the 2005 SPE Annual Technical Conference and Exhibition, Dallas, 9-12 October.

7. Tucker, M.E. and Bathurst, R.G.1990. *Carbonate Diagenesis*, Oxford: BlackWell Scientific Publication.

8. Wilson, J.L. 1975. *Carbonate Facies in Geologic History*. Berlin: Springer-Verlag.

9. Ahr, W.M. 1973. The Carbonate Ramp - An Alternative to the Shelf Model. *Trans.,* Gulf Coast Association of Geological Societies Vol. **23**: 221-225.

10. Lee, W.J., Rollins, B. J. and Spivey, J.P. 1997. *Well Testing*, Textbook Series, SPE, Richardson, Texas: 151-154.

11. Correa, F. A. and Ramey, H.J. 1987. A Method for Pressure Buildup Analysis of Drillstem Tests. Paper SPE 16802 presented at the SPE Annual Technical Conference and Exhibition, Dallas, 27-30 September.

12. Warren, J.E and Root, P.J. The Behavior of Naturally Fractured Reservoirs. SPE Journal (Sept. 1963) 52-53.

13. Bahar, A. and Kelkar, M. 1998. Journey From Well Logs/Cores to Integrated Geological and Petrophysical Simulation: A Methodology and Application. Paper SPE 39565 presented at the 1998 SPE India Oil and Gas Conference and Exhibition, New Delhi, 17-19 February.

14. Aufricht, W.R. and Koepf E.H. 1957. The Interpretation of Capillary Pressure Data from Carbonate Reservoirs. Revised Manuscript SPE 826-G available from SPE, Richardson, Texas.

15. Carter, R.D. and Tracy, G.W. 1960. An Improved Method for Calculating Water Influx, *Trans.,* AIME **219**, 156.

16. Wattenbarger, R.A. 2006. Advanced Reservoir Engineering class notes, Texas A&M University, College Station.

17. Peaceman, D.W. 1977. Interpretation of Well-Block Pressures in Numerical Reservoir Simulation. Paper SPE 6893 presented at the SPE-AIME 52nd Annual Technical Conference and Exhibition, Denver, 9-12 October.

18. Gang, T. and Kelkar, M. 2006. Efficient History Matching in Naturally Fractured Reservoirs. Paper SPE 99578 presented at the 2006 SPE/DOE Symposium on Improved Oil Recovery, Tulsa, 22-26 April.

19. Willhite, G. P. 1986. *Waterflooding*, Textbook Series, SPE, Richardson, Texas, 36-39.

20. Economides, M. J., Oligney, R. E. and Valko, P. 2002. *Unified Fracture Design: Bridging the Gap Between Theory and Practice*, 21. Alvin, Texas: Orsa Press.

21. Valko, P. and Economides, M. 1995. *Hydraulic Fracture Mechanics*, New York: Wiley Chichester.

APPENDIX A

DIAGRAMMATIC REPRESENTATION OF THE MONUMENT NORTHWEST FIELD

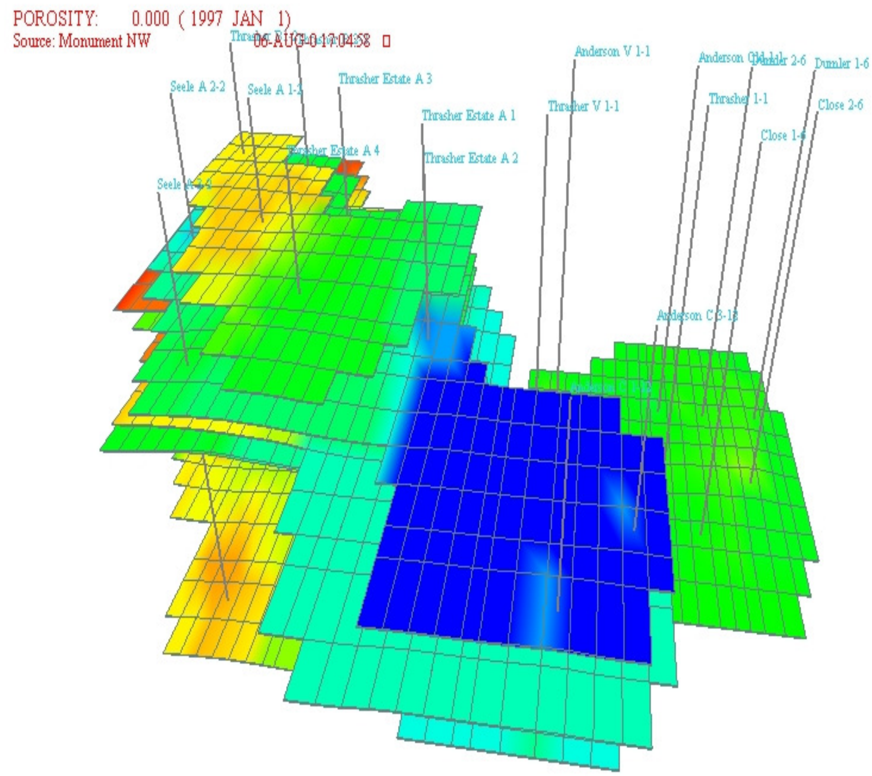

Figure A1: 3D reservoir model of the Monument NW field showing wells. The blue areas show acreage extension to account for two Anderson Wells perforated into those zones.

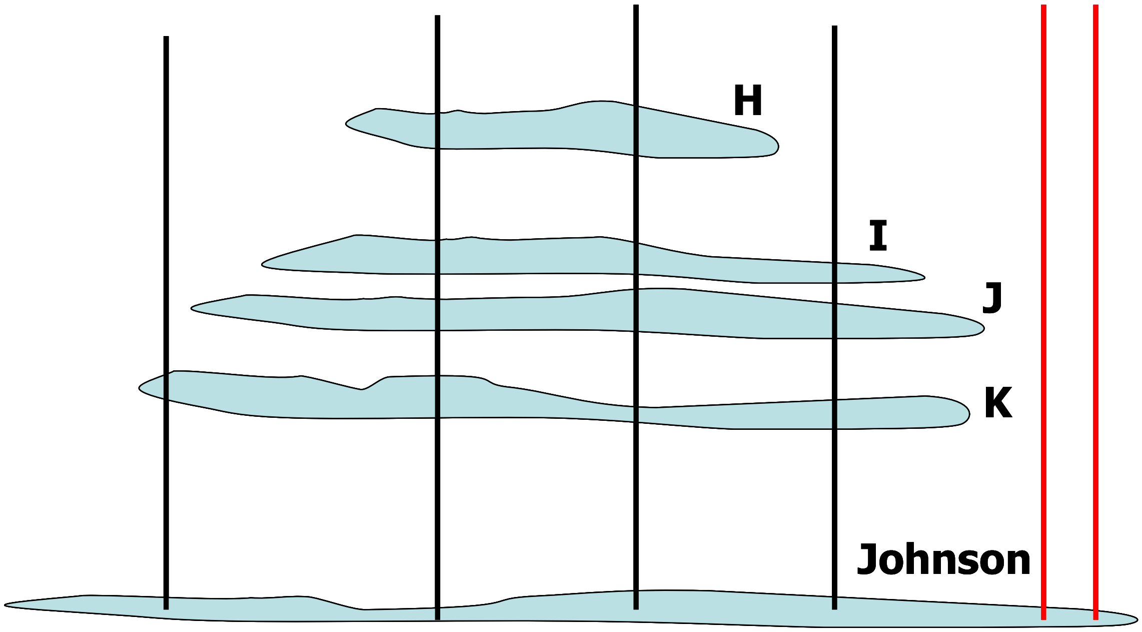

Figure A2: 2D representation of the Monument NW field. The black wells (not completely shown) are the wells modeled in the reservoir model developed. The red wells are wells in other sections which have been producing earlier from the Johnson structure.

APPENDIX B

WELL PRODUCTION AND PRESSURE MATCH FOR WELLS MODELED IN THE MONUMENT NORTHWEST FIELD.

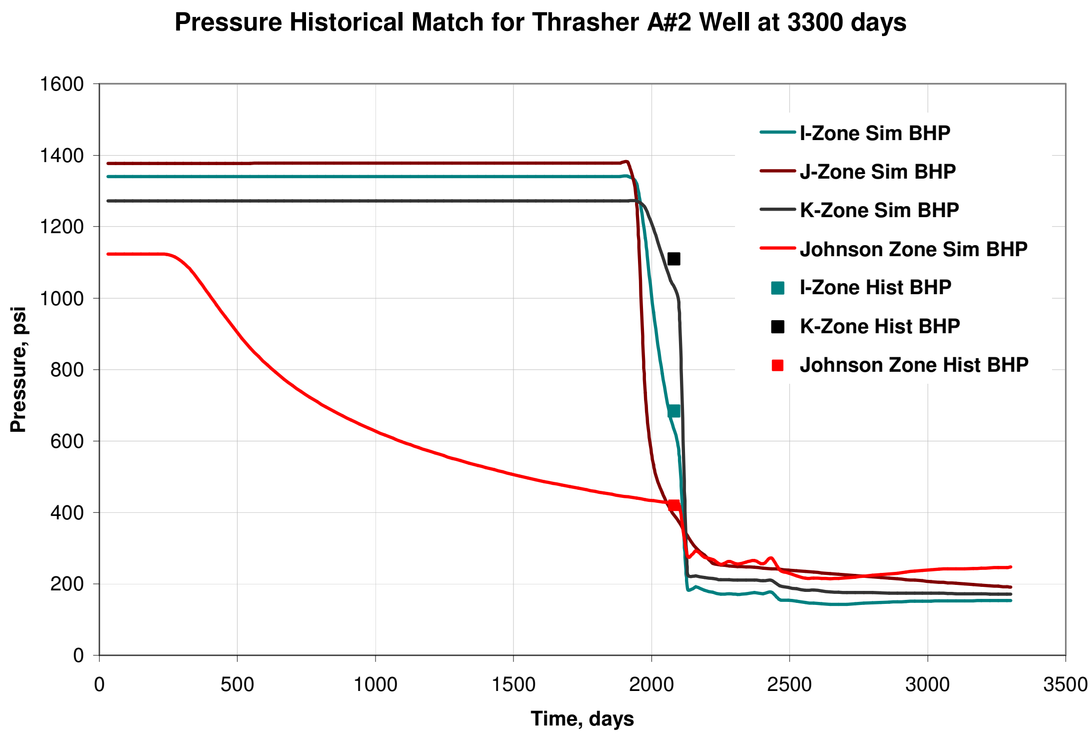

Figure B1: Pressure history match for Thrasher A#2 well. We observe a good match for this case.

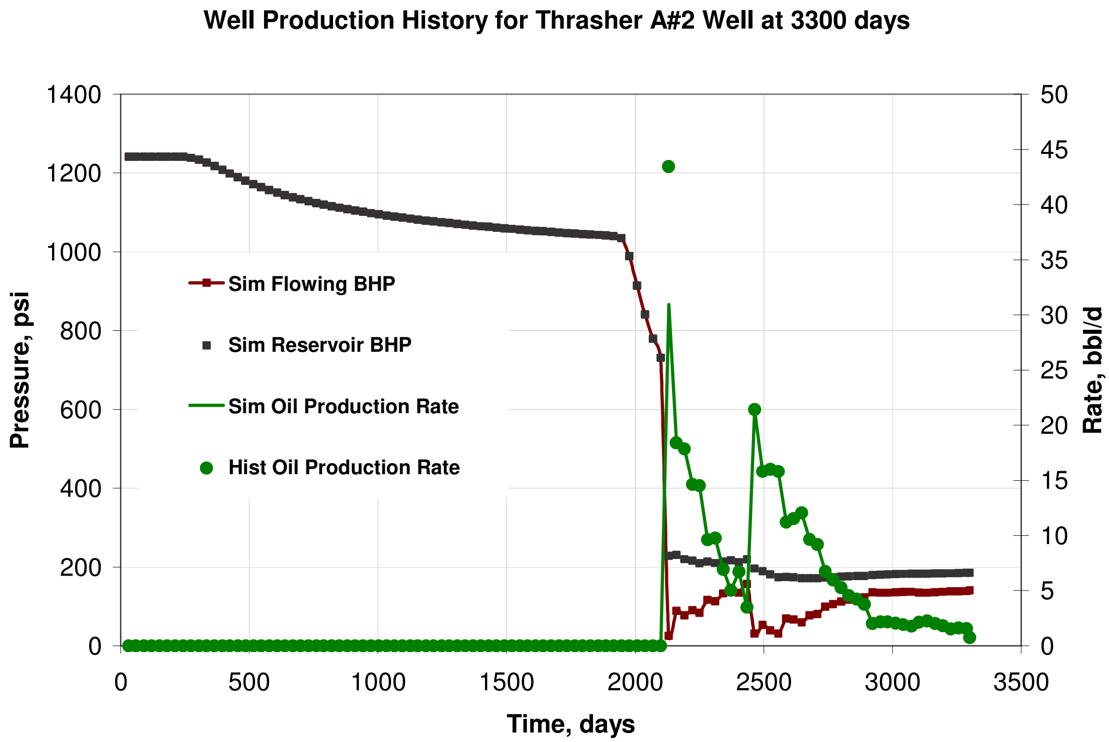

Figure B2: Well production history for Thrasher A#2 well. The flowing BHP is quite high for this case and a further skin allocation or permeability reduction would make the oil rate match trail off.

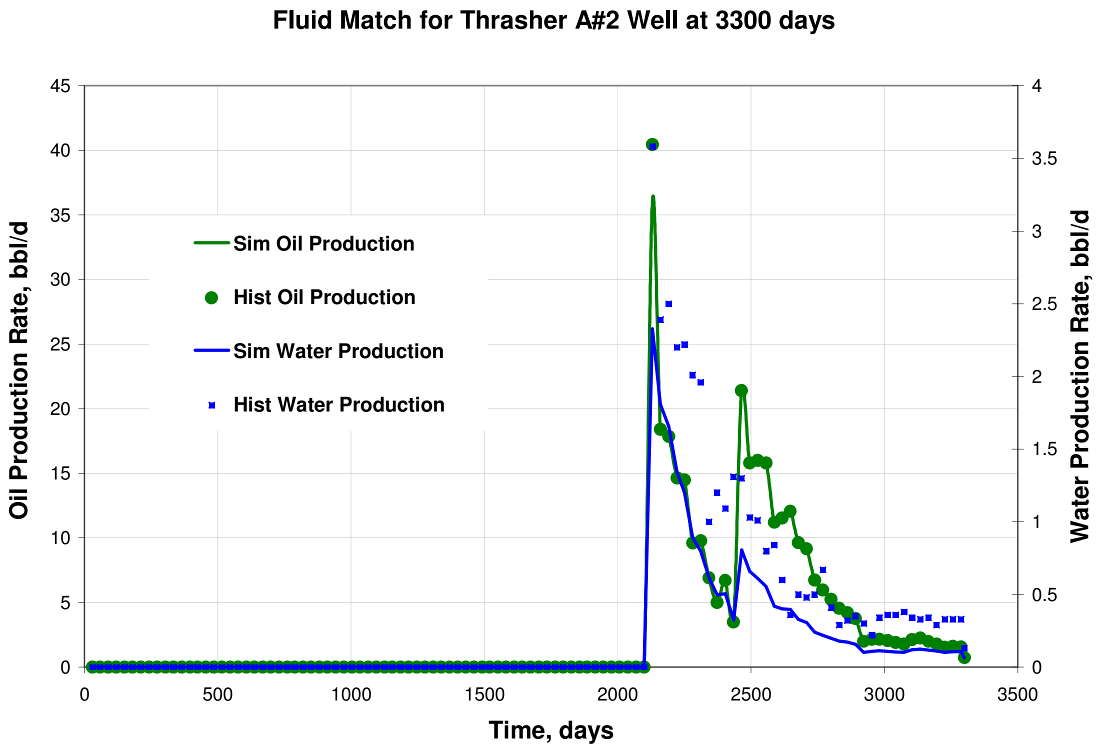

Figure B3: Fluid match for Thrasher A#2 well. Oil match is very good and the water match is reasonable.

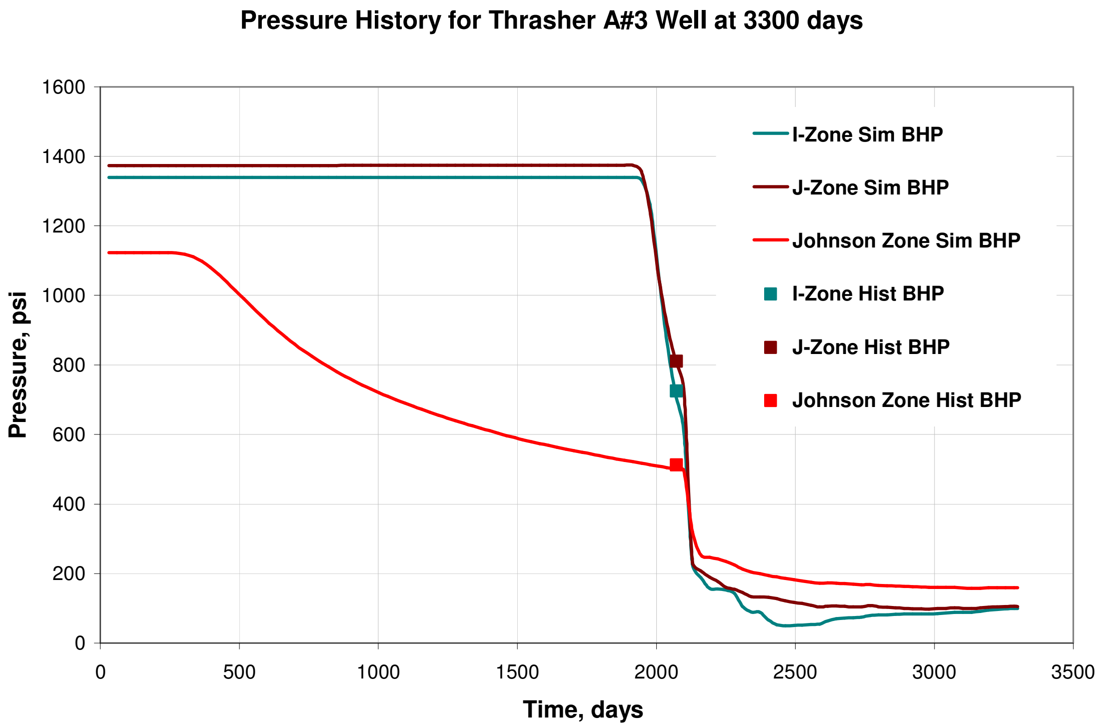

Figure B4: Pressure history match for Thrasher A#3 well. The pressure match on this well is very good.

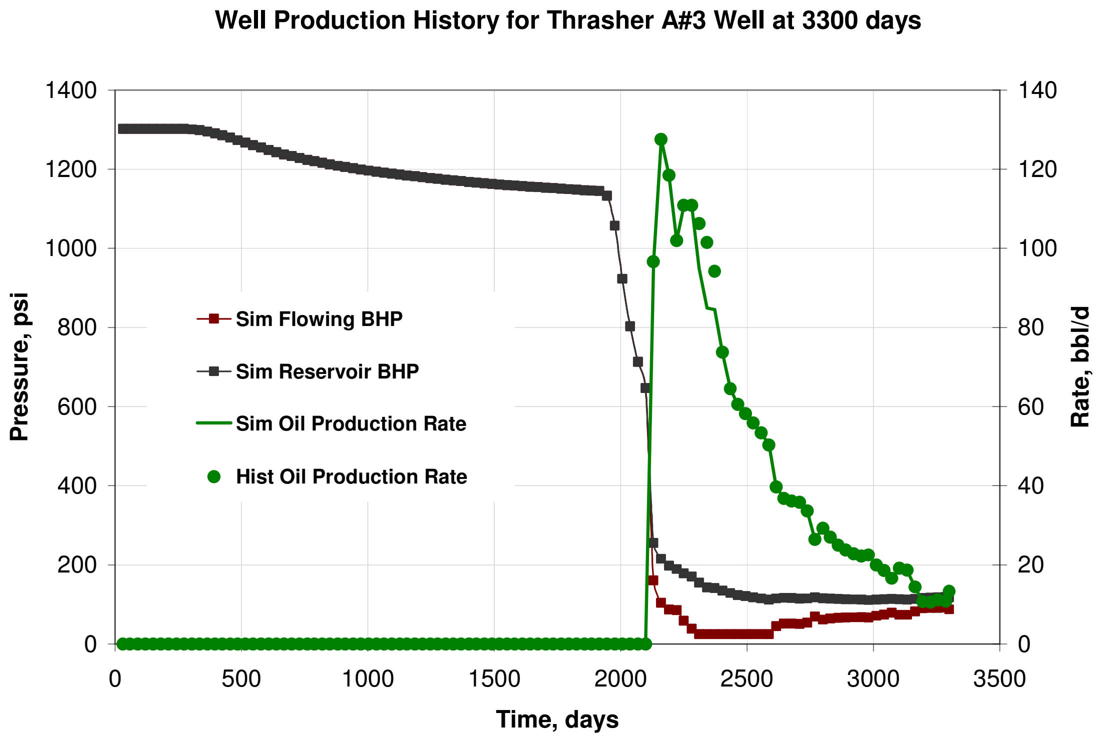

Figure B5: Well production history for Thrasher A#3 well. We observed the well being pumped off and this is closely simulated by the reservoir model which trails off a bit on the oil production match.

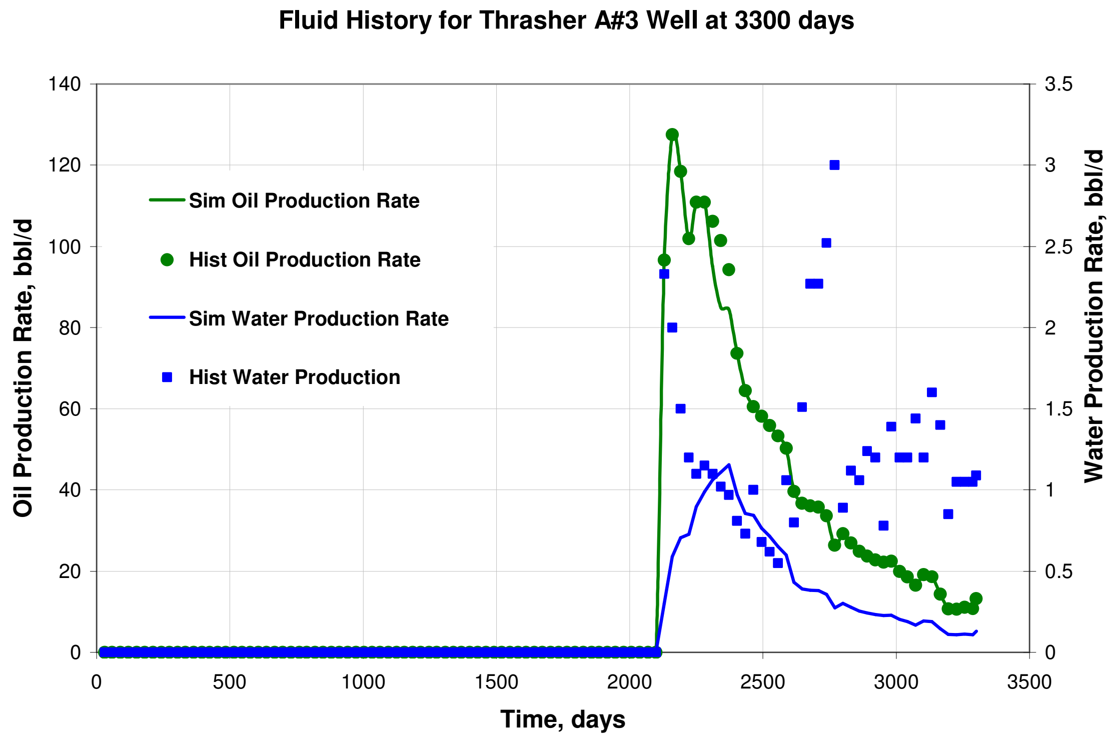

Figure B6: Fluid history match for Thrasher A#3 well.

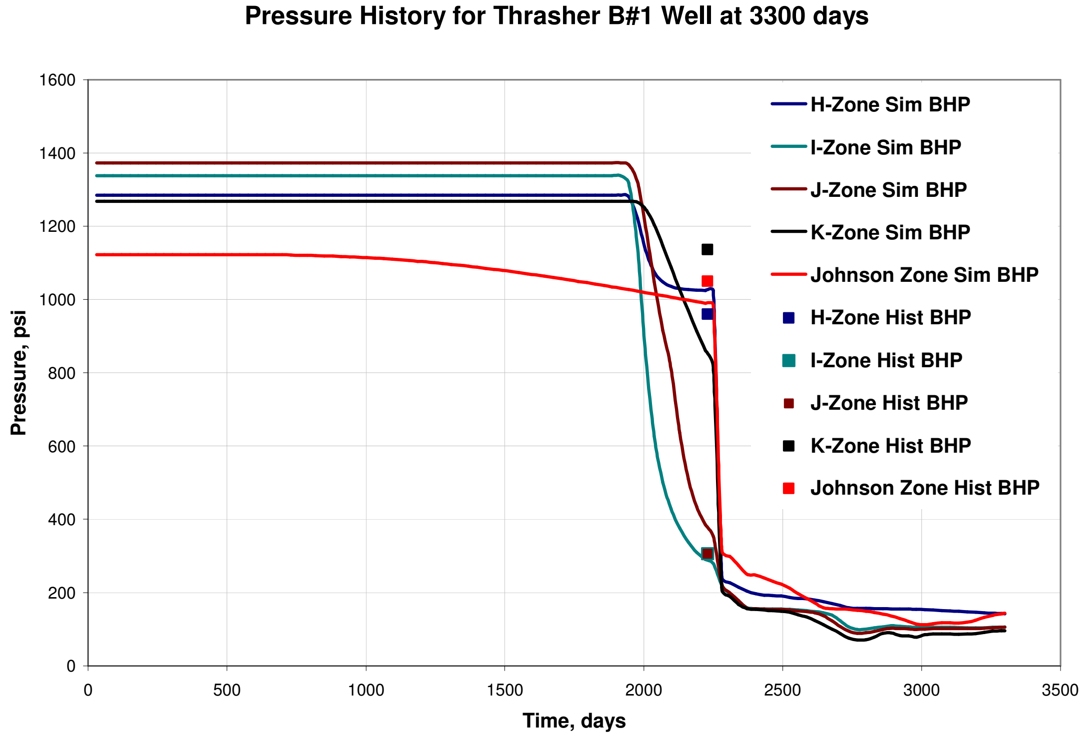

Figure B7: Pressure history match for Thrasher B#1 well. We observe high pressures at most of the zones including the H-Zone with the aquifer.

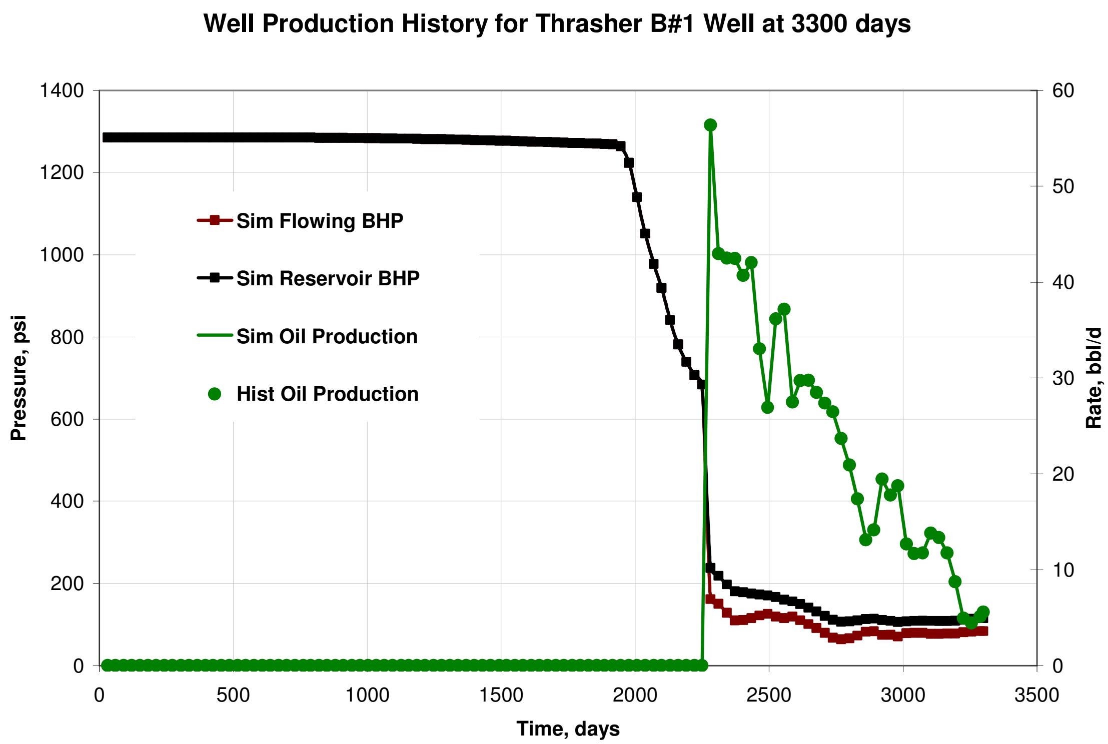

Figure B8: Well production history for Thrasher B#1 well.

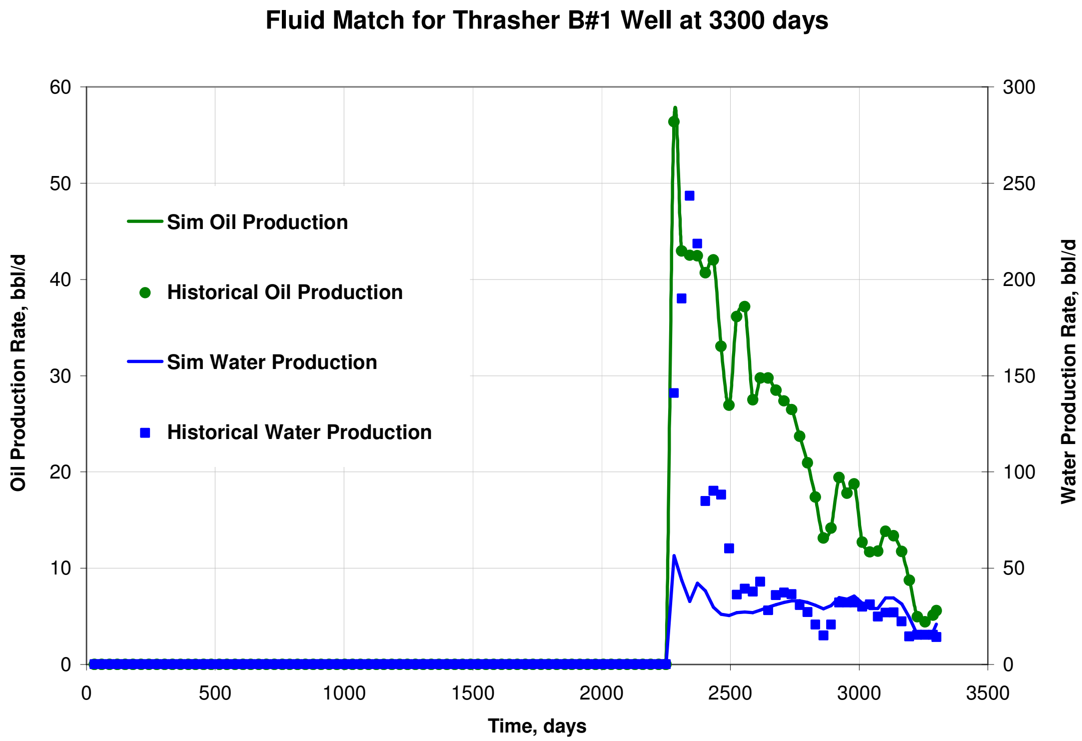

Figure B9: Fluid history match for Thrasher B#1 Well. We see high water production from this well due to the H-Zone aquifer.

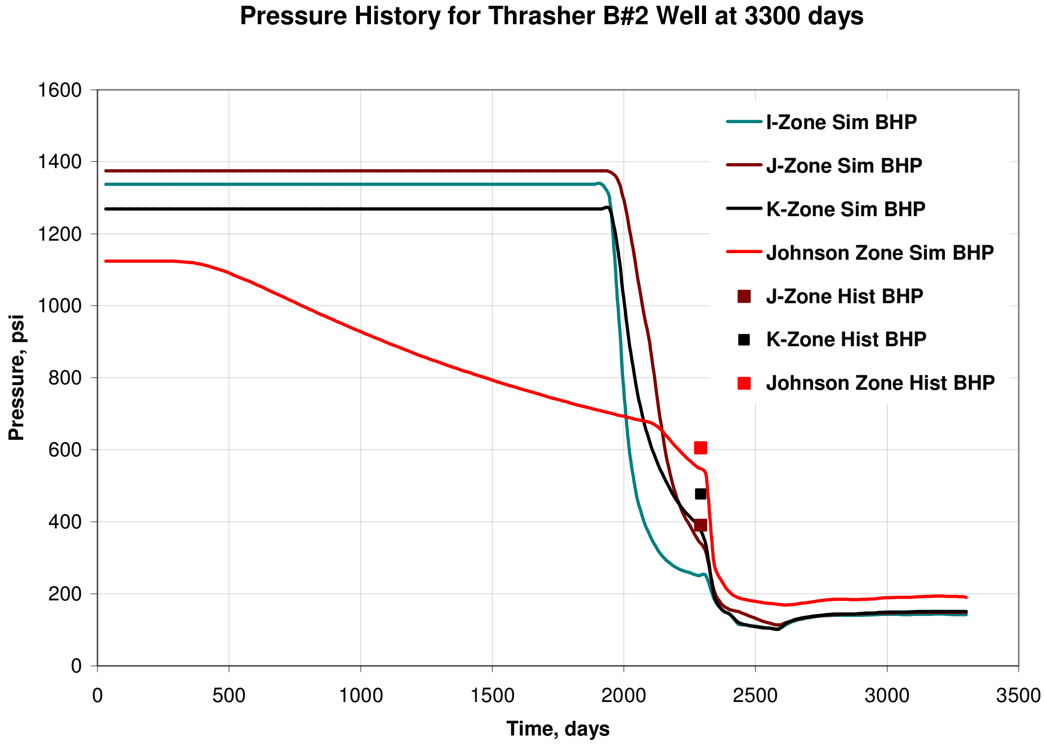

Figure B10: Pressure history match for Thrasher B#2 well.

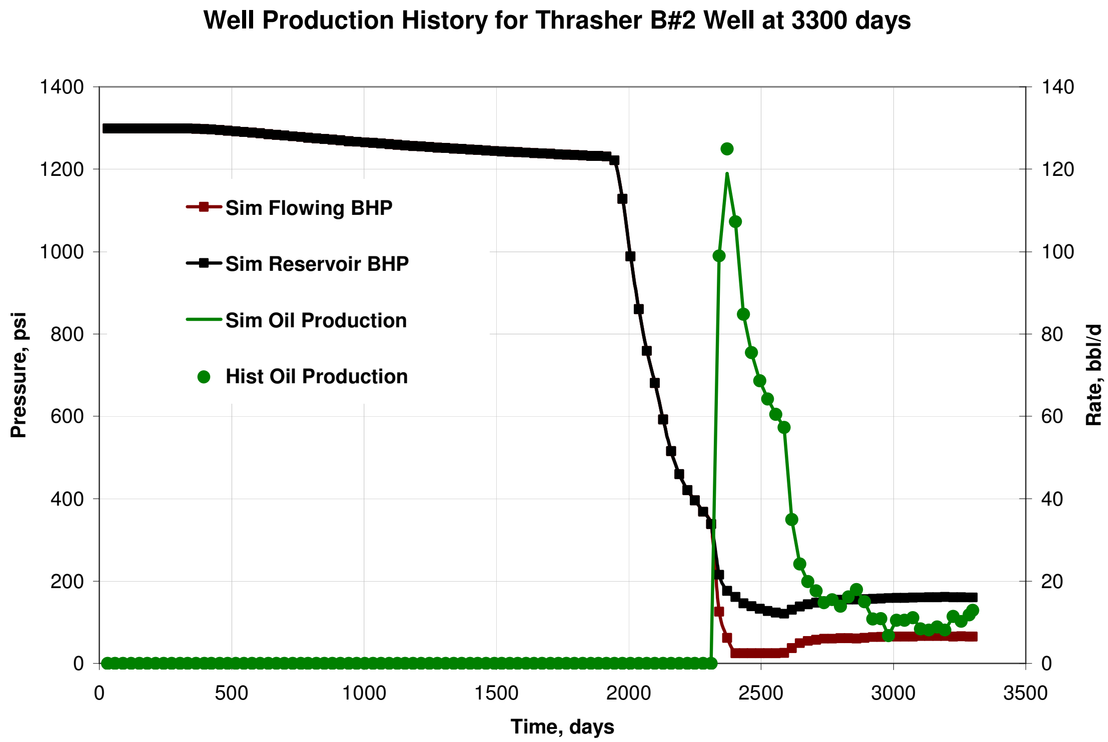

Figure B11: Well production history for the Thrasher B#2 well.

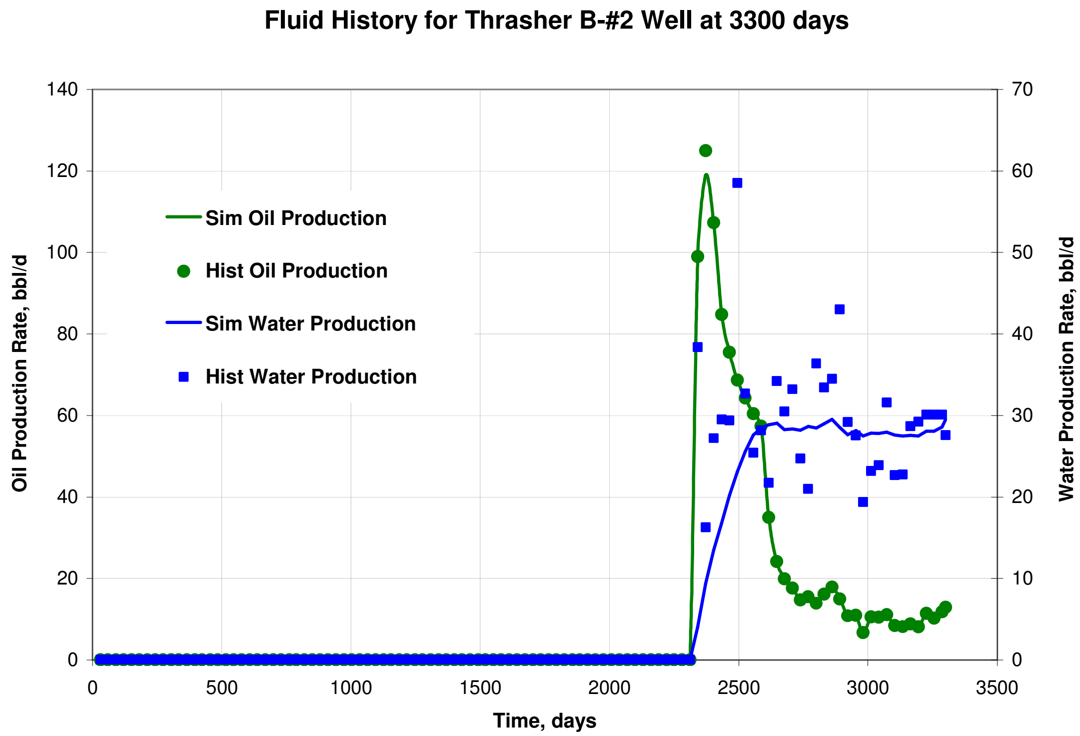

Figure B12: Fluid match for the Thrasher B#2 well.

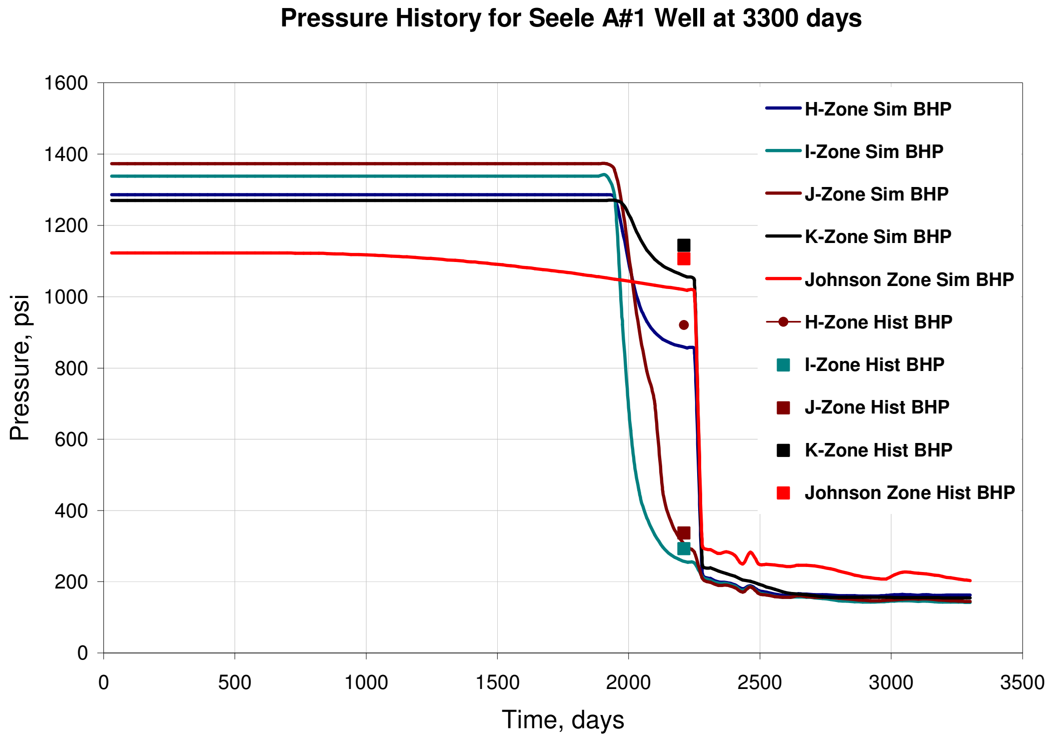

Figure B13: Pressure history match for Seele A#1 well.

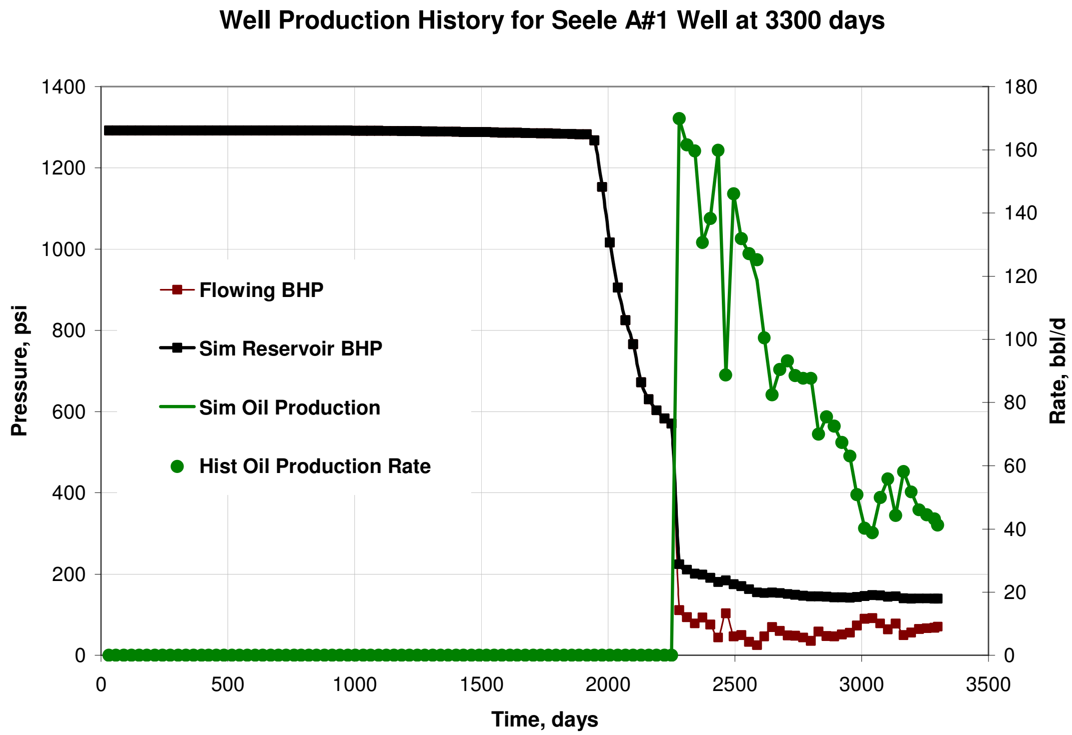

Figure B14: Well production history for Seele A#1 well.

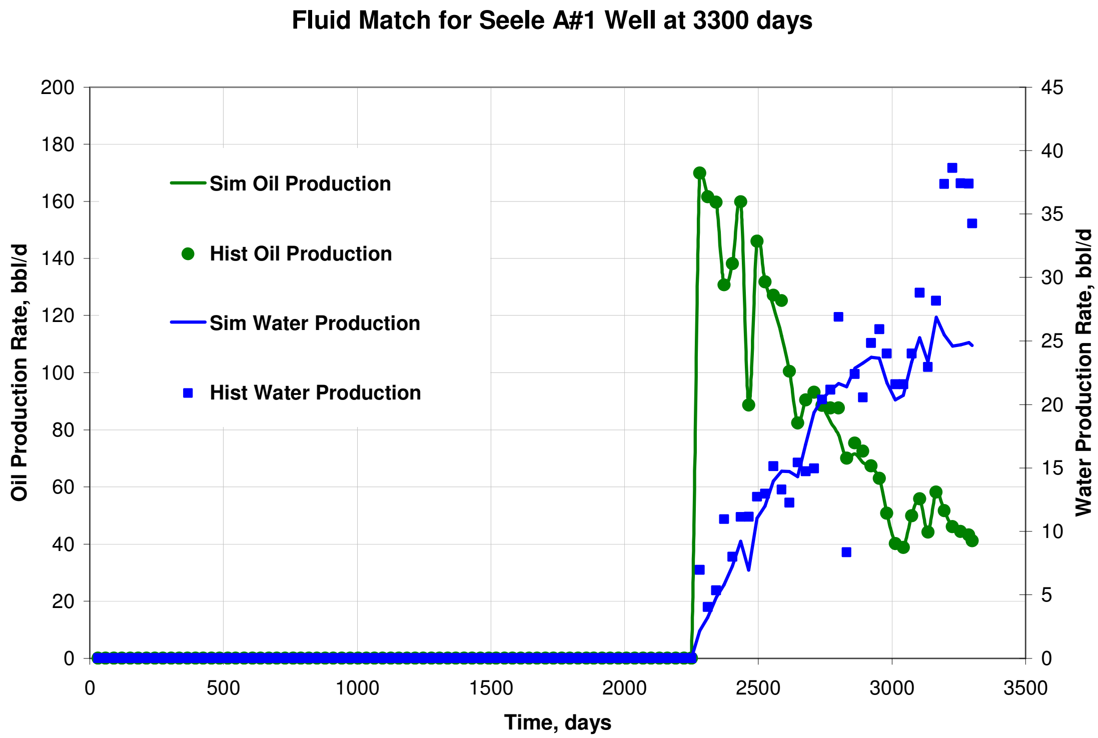

Figure B15: Fluid match for Seele A#1 well. We observe increasing water production mainly due to the H-Zone aquifer.

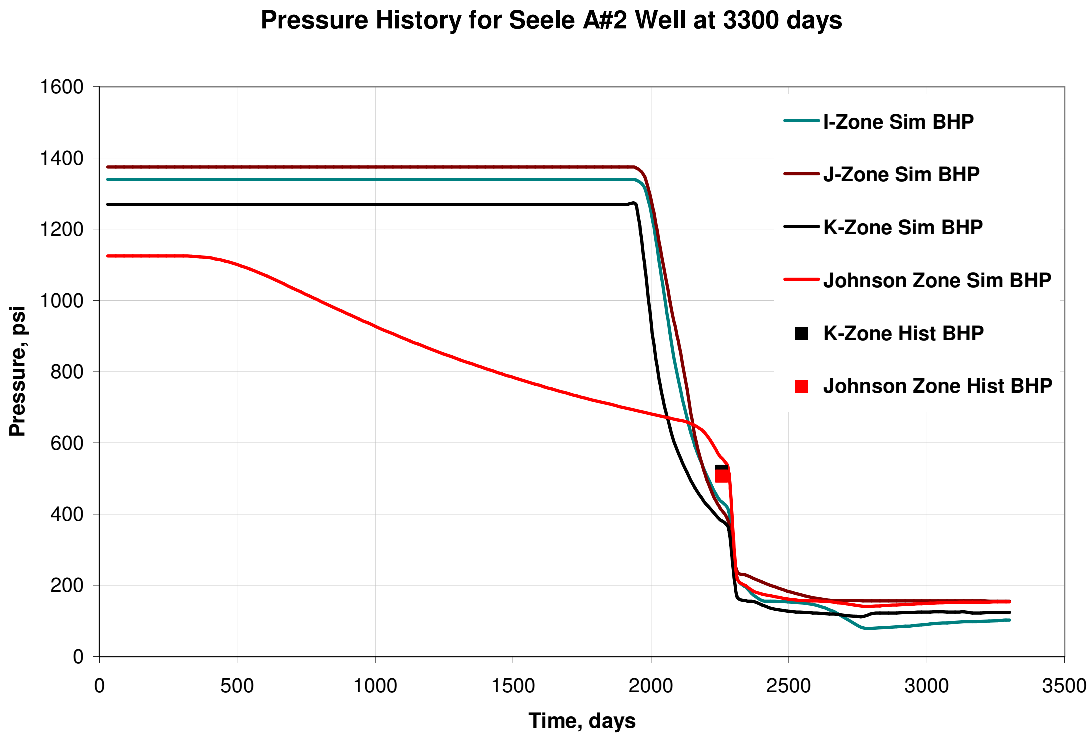

Figure B16: Pressure history match for Seele A#2 well.

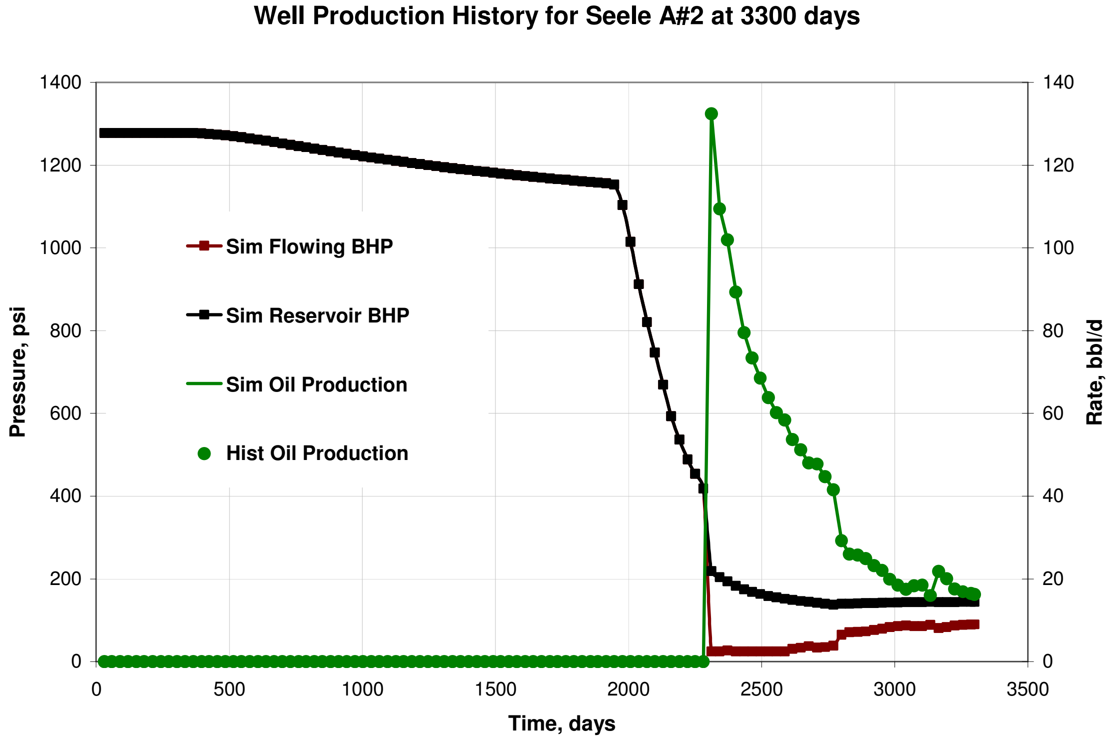

Figure B17: Well production history for Seele A#2 well.

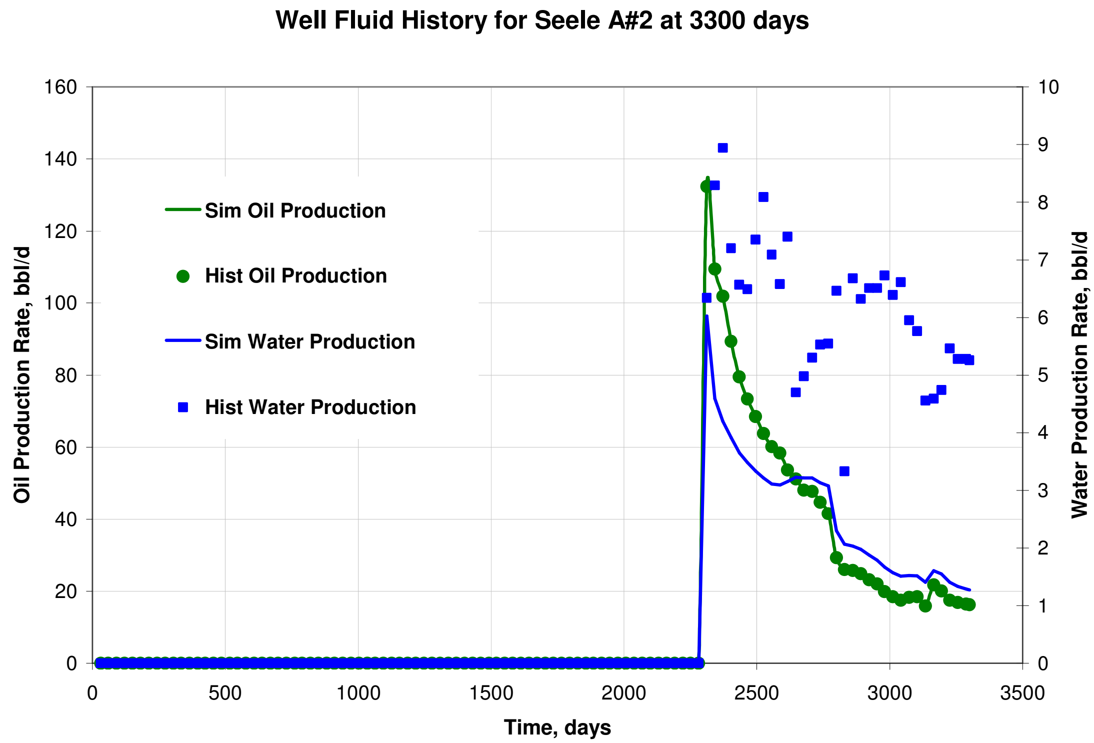

Figure B18: Fluid history match for Seele A#2 well.

VITA

Moses Asuquo Nduonyi received his Bachelor of Engineering degree in petroleum engineering from the University of Port Harcourt in Nigeria. He entered into the petroleum engineering program at Texas A&M University in September 2005 and received his Master of Science degree in December 2007. His research and work interests include reservoir modeling and pressure transient analysis with a view to enhanced oil recovery.

Mr. Nduonyi may be reached at iValue Consulting, 1501 Holleman Drive College Station, TX 77840. His email is moses_asuwko@tamu.edu.